공학석사학위 논문

Study on electrokinetics behavior in nanochannels with all around gate electrode

All around gate가 삽입된 나노채널에서의 electrokinetics현상에 관한 연구

2014년 8월

서울대학교 대학원

재료공학부

Tian Guang Jin

Study on electrokinetics behavior in nanochannels with all around gate electrode

A DISSERTATION SUBMITTED TO

DEPARTMENT OF MATERIAL SCIENCE AND ENGINEERING

SEOUL NATIONAL UNIVERSITY

FOR THE DEGREE OF

MASTER

Tian Guang Jin

August 2014

`

Abstract

Due to the increased sophistication of cleanroom technology, the device could be implemented with nanoscale by people and among of new - born things, nanofluidics is one of them. Nanofluidics is a combined research field of “Nanotechnology” and “Fluidics”, has recently focused in the last decade. Thus, the nanofluidics exhibits respective properties of “Nanotechnology” and “Fluidics”, which was utilized to several potential applications such as high – throughput bio – health application, clean energy generation, and other alternatives applications.

Nanofluidics is paid an attention to manipulate the charged species in electrolyte environment, where bio – molecule is the most concerned about. Most of bio – molecules are existed in electrolyte environments and their size is about sub 10nm range, therefore a well – defined nanoscale platform was highly required to analyze the tiny bio-molecules with electrolyte conditions. Also, if want to achieve the aim of bio-molecules manipulation, control of ion transport is first step.

In this thesis, we fabricated all – around gated IFET (Ionic Field Effect Transistor) which could control the ion transport in nanofluidic devices. On the view of nanochannel fabrication, we developed fabrication method of sub 10 nm nanochannels with transparent AZO (Al – doped Zinc Oxide) gate electrode. And we utilized high dielectric constant material Al_2O_3 (9) instead of conventional SiO_2 (4.5). Furthermore, the surface charge density of Al_2O_3 was only -1.8 mC/m^2, almost neutral polarity. Therefore, the device exhibited ambipolar behavior in I_D vs V_G (Ionic current vs Gate voltage) relation, compare to conventional IFET (Ionic Field Effect Transistor). The reason of ambipolar behavior came from the gate structure and inherent surface charge density. Because of all – around gate structure, the gate voltage could induce more than 5 times extra charge at surface, and the almost neutral surface charge could reverse the polarity

`

more easily. Finally, we measured the ionic current at wide range of electrolyte concentration (10^{-5} ~ 10^{-2} M) with gate voltage variation to verify the gate effect.

The experimental ambipolar results were validated with COMSOL simulation. And the fringing effect and counter ion condensation effect was proved indirectly with partially gate embedded IFET (Ionic Field Effect Transistor).

Finally, the material of gate electrode AZO (Al – doped Zinc Oxide) is transparent, thus the flow of ions or bio – molecules are controlled electrically, observed optically at the same time. That point of view, this device will be new concept nanofluidic devices for bio – molecules analysis.

Keywords: Nanofluidics, Nanochannel, Ionic field effect transistor

Student number: 2012-23926

`

Table of Contents

`

`

List of Figures

Chapter 1

`

Chapter 2

`

Chapter 3

`

`

Chapter 4

`

Chapter 5

`

Chapter 1. Introduction

`

1. Introduction

1. Nanofluidics and electrokinetics

With the development of technology for sophistication of cleanroom equipment, and requirement of precise biological application; a new research field referred as nanofluidics was formed. [1], [2] ***Nanofluidics*** is study fluidic dynamics in restricted channel of the size or dimension is below 100nm. And if the physical scaling lengths of the fluid takes down to the nanofluidics level which is defined above, the fluids have unique phenomena is referred as perm – selectivity and which only allow the counter – ion to exist within a certain thickness from the solid / liquid interface. And this thickness is represented by characteristic length and named by Debye screening length. Furthermore, the unique phenomenon has not been shown never in any other situation even microfluidics. [3]

Except for concept of nanofluidics, we should understand another new concept referred as electrokinetics, when we fabricate nanofluidic devices for actual applications. Analogical to electronic devices, the nanofludic devices are operated by electrical power and focus on concerning of charged species transportation phenomena in the nanofluidic devices. Therefore, all phenomena or result obtained from nanofludic devices should be analyzed in term of electrokinetics. ***Electrokinetics*** refers to the use of electric fields to exert electrostatic forces on charged or polarizable fluids and suspended particles, which in turn induces the motions of fluids and particles. [4]

For sufficiently utilize the unique phenomena of perm – selectivity, the physical dimension of the fluidic device should be comparable to level of defined nanofluidics. And depending on the configuration of nanofluidic devices, it is divided into three types, including nanochannel, and nanopore [5], [7]. So that over past few years, the previous research paid attention to utilize nanofluidic devices as a tool for clean energy harvesting [6], desalination of sea water [7], and biological applications [8]. And according to the situation or application, appropriate devices

`

should be selected by researches. Because of membrane structure, nanopores are more sensible than nanochannels, hence, nanopores are used for detector or sensor of charged bio – molecules such as DNA, RNA, and proteins [9], [10]. In contrast, nanochannels have higher aspect ratio than nanopores; nanochannels have better charged species selectivity than nanopores [11]. For instance clean energy harvesting and desalination of sea water, selectivity is key issue for these applications. Energy harvesting needs filtering only one species ion (cation or anion) to pass through the nanochannels and generate electric current, and desalination of sea water itself is based on selectivity. Except for detector or sensor of charged bio – molecules such as DNA, RNA, and proteins, DNA stretching is also hot issue for bio – application in nanochannel [12], [13].

2. Role of surface charge in nanofluidic devices

Because of large surface – to – volume ratio of nanofluidic devices, the surface charge density plays the most important role in the nanofluidic devices to govern the overall flows in nanofluidic devices. Therefore, modulating the surface charge density itself has great implications. In order to the purpose of fabricating tunable nanofluidic devices, there have been developed four kinds methods by previous researchers. First, surface charge was formed due to hydrolyzed reaction between solid / liquid interface. The pH value of electrolyte determines the surface charge density directly [14]. Second, surface treatment was deal with given chemical and it can modify the inner surface of nanofluidic devices in order to change the surface charge density even switch the polarity of surface charge [15]. Third, visible light can be used to control the surface charge density of nanofluidic devices [16], and this method shows big difference between the two front methods. Compare with changing pH value of electrolyte and surface treatment, optical tuning is active method. The last one is the IFET (Ion Field Effect Transistor) [17]. In contrast with optical tuning method, IFET (Ion Field Effect Transistor) uses external gate voltage to modulate the surface charge density instead of light shining. So IFET

`

(Ion Field Effect Transistor) is the conventionally and widely used method in the field of nanofluidic devices.

3. IFET definition and conventional IFET

What is the IFET (Ion Field Effect Transistor)? Analogy to electronic device, nanofluidics device also can be configured to logic circuit – diode, transistor etc. The surface charge of nanofluidic devices can be manipulated by the gate voltage.

However, the conventional dielectrical layer of IFET (Ion Field Effect Transistor) was basically SiO_2 or nanoporous resin because of fabrication method and low dielectric constant [18], [19], [20]. Although these materials had merits in fabricating like mass production, uniformity of each device; they hardly overcome the fatal disadvantage which is the high surface charge density. The aim of fabricating IFET (Ion Field Effect Transistor) is to manipulate the surface charge density with gate voltage; however, if the inherent surface charge density is too high, it will require relatively higher gate voltage to obtain the visible variation of ionic current. In addition, higher gate voltage causes the higher leakage currents, and the gate voltage reach to dielectric breakdown voltage level, and then devices will fail.

And high surface charge density engendered unipolar behavior with I_{SD} versus V_G graph (plot the source drain current versus gate voltage). [18], [19], [20] A unipolar behavior occurs for the extra induced surface charges by gate voltage are not able to overcome the polarity of inherent ones. Coupled with limitation of fabrication method, only planar gate electrode was installed for nanochannel type IFET (Ion Field Effect Transistor), when compare to nanopore type IFET (Ion Field Effect Transistor).

4. Modified conventional IFET (Ion Field Effect Transistor)

From the above paragraph, several limitations can be enumerated by us as follows: inherent surface charge density, dielectric constant of oxide, and gate electrode structure. The latter two

`

terms in the limitations are fixed already when the devices are fabricated and there will be permanent, therefore, there are intrinsic properties. Oppositely, inherent surface charge density can be modulated by pH conditions of electrolyte or surface treatment case by case and it is independent with material and structure of constituting devices so it is extrinsic property.

In order to improve the efficiency of conventional IFET (Ion Field Effect Transistor), presenting paper utilized the extrinsic property – modulating inherent surface charge density with pH conditions of electrolyte or surface treatment.

Youn-Jin Oh *at al* reported that if the pH values of electrolyte can be controlled at point of zero charge level, the conventional IFET (Ion Field Effect Transistor) also exhibits ambipolar behavior. In this paper, they showed direction of electrolyte flow (fluorescence dye signal) with gate voltage polarity change. The direction of electrolyte flow (fluorescence dye signal) changed to the opposite direction when the polarity of gate voltage is from < - > to < + >, which phenomena prove the gate voltage can overcome the inherent polarity of surface charge. [21] The second paper shows similar image at microchannel. Anyway, it is the fact that external voltage – induced charge can conquer the original ones. [22]

Surface treatment with surfactant also was mentioned; Rong Fan *at al* reported the effect of surfactant. The surfactant decreased the inherent surface charge density gradually, after 2 days from surface treatment, the surfactant played role as same as electrolyte pH condition at point of zero charge. Amazingly, after 4 days from surface treatment, the surfactant overturned the status from inherent < - > surface charge to < + > surface charge. Another paper showed the surfactant could reduce the surface charge density less than 0.2 mC/m^2. Because the surface was almost zero charged, only 1 V (absolute value) was sufficient to operate the device. [23] In comparison with other paper, author experimented with protein instead of pure potassium chloride solution, however, in the point view of controlling the charged species, which is an identical phenomenon. [24]

`

5. Suggestion

So far, many researchers focused on efficiency improvement of IFET (Ion Field Effect Transistor). The extrinsic property of IFET (Ion Field Effect Transistor) could be modulated with several methods such as changing pH value of electrolyte, or surface treatment. But neither changing pH value of electrolyte nor surface treatment is satisfactory methods because they were all passive methods.

And intrinsic property of IFET (Ion Field Effect Transistor) was dependent with gate oxide material and gate electrode structure, so we were able to use other material with higher dielectric constant and low surface charge density material Al_2O_3 instead of conventional SiO_2. Figure 1 – 5 shows the reason for choose of Al_2O_3. For limitation of gate electrode structure, compared the capacitance of planar type to cylindrical type with same contact area, length, and dielectric constant, the cylindrical type works more effective at same gate voltage because all of the surface of nanochannel can be affected by gate voltage. Moreover, the similar 3D FinFET type structure was been researched in solid state electronic device. [Figure 1 – 6]

In this article, we suggest an ideal and perfect structure for IFET (Ion Field Effect Transistor) is Based on the above consideration. The suggested IFET (Ion Field Effect Transistor) should be all – around (cylindrical type) gate structure, neutral surface charged dielectric material with high dielectric constant, and the dimension of nanochannel is as small as possible. We fabricated the nanochannels device with 15 nm diameter and 20 μm lengths, and the gated region is 10 μm lengths at the center of whole 20 μm nanochannels. The Al_2O_3 was used as gate oxide, and the gate structure was desired all – around type. Finally, the gate electrode material was TCO (Transparent Conducting Oxide), so we also could obtain the optical signal according to gate voltage changes; it is as well as gigantic merit for IFET (Ion Field Effect Transistor).

`

6. Reference

[1]. Jan C. T. Eijkel et al., Microfluid Nanofluid, **1**, 249 – 267, (2005).

[2]. W. Sparreboom et al., New Journal of Physics **12**, 015004, (2010).

[3]. Reto B. Schoch et al., Rev. Mod. Phys., **80**, 839 – 883, (2008).

[4]. Shizhi Qian – Electrokinetic particle transport in micro / nanofluidics – version date:20120409

[5]. Patrick Abgrall et al., Analytical Chemistry, 80(7), 2326–2341, (2008).

[6]. Xie. Y. B et al., Appl. Phys. Lett. **93**, 163116, (2008).

[7]. Kim. S. J et al., Nature Nanotechnology, **5**, 297 – 301, (2010).

[8]. Cess Dekker, Nature nanotech., **2**, 209 – 215, (2007).

[9]. Stefan W. Kowalczyk et al., Nano Lett., **12(2)**, 1038−1044, (2012).

[10].Wenhong Li et al., ACS Nano., **(7)5**, 4129–4134, (2013).

[11].Ivan Vlassiouk et al., Nano Lett., **8(7)**, 1978 – 1985, (2008).

[12].Yoori Kim et al., Lab Chip, **11**, 1721–1729, (2011).

[13].K.D. Park et al., Microelectronic Engineering **86**, 1385–1388, (2009).

[14].Meni Wanunu et al., Nano Lett., **7 (6)**, 1580 –1585, (2007).

[15].Rohit Karnik et al., Nano Lett. , **7(3)**, 547 – 551, (2007).

[16].Nicolas Di Fiori et al., Nature Nanotechnology, **8**, 946 – 951, (2013).

[17].Gajor S A et al., J. Electrochem. Soc., **139**, 2833 – 2840, (1992).

`

[18].Gaun, W et al., Nat. Commun, **2**, 506, (2011).

[19].U.Vermesh et al., Nano Lett., **9(4)**, 1315, (2009).

[20].R. Fan et al., Nature Materials, **7**, 303, (2008).

[21].Youn-Jin Oh et al., Lab Chip, **9**, 1601–1608, (2009).

[22].Schasfoort R. B. M et al., Science, **286**, 942 – 945, (1999).

[23].Fan et al., Phy. Rev. Lett., **95**, 086607, (2005).

[24].Rohit Karnik et al., Applied Physics Letters, 88, 123114 (2006).

[25].S. Nam et al. Nano Lett., **10 (9)**, 3324–3329, (2010).

[26].S. Nam et al. Nano Lett., **9 (5)**, 2044–2048, (2009).

`

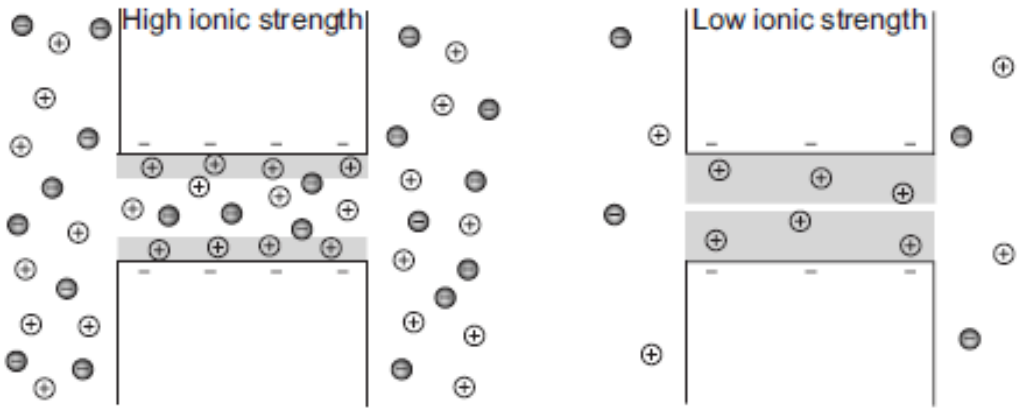

Figure 1 – 1: Concept of Nanofluidic devices.

EDL (Electrical double layer), shaded in gray at high ionic strength, it is thin, allowing co-ions and counter ions to pass through the nanochannel. At low ionic strength, the EDL thickness increases, resulting in a counter ion-selective nanochannel. [3]

`

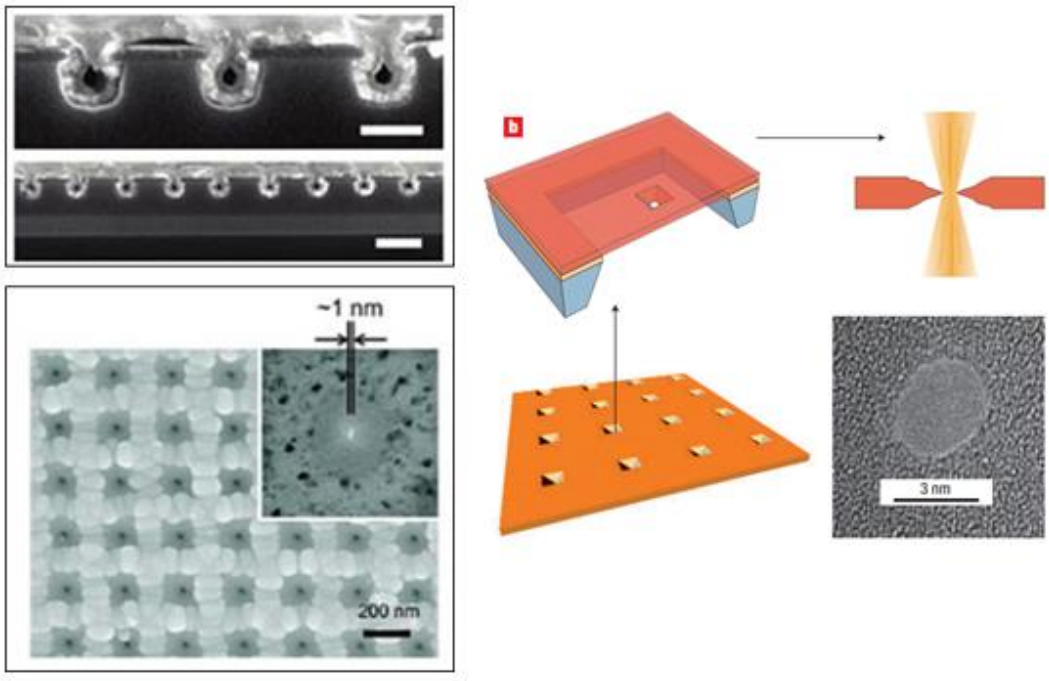

<a> <b>

Figure 1 – 2: Image of nanochannel and nanopore

a. Geometrical defined the nanochannel devices and naopore devices. Nanochannel devices had high aspect ratio, compared with nanopore devices. Nanochannel devices were named 1D nanofluidic devices and naopore devices were named 0D nanofluidic devices. [25, 26]
b. Schematic image of solid state naonopore. Nanopore was consisted with one layer nanometer thickness membrane. [7]

`

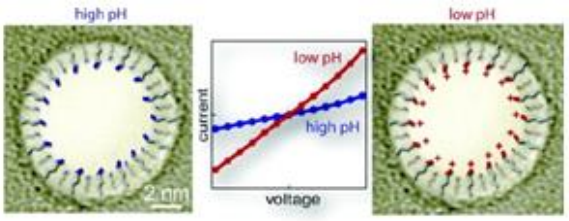

<a>

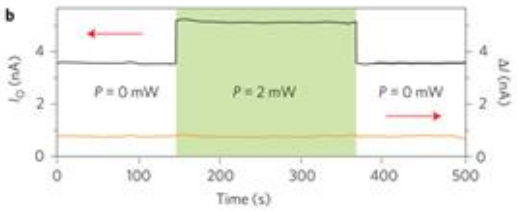

<b>

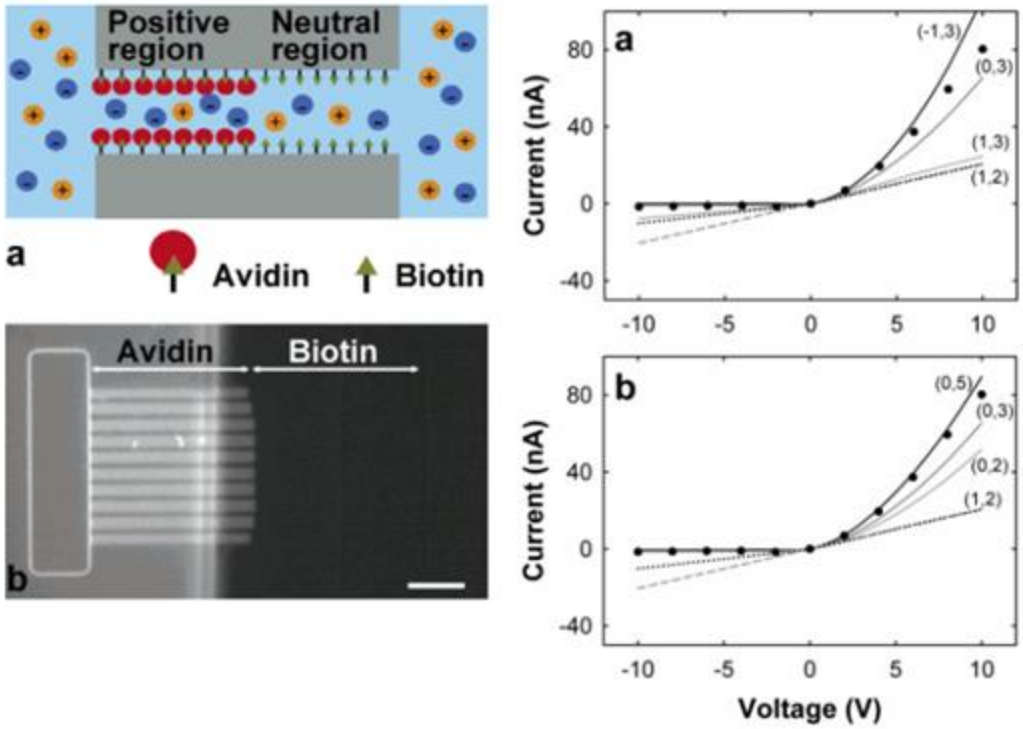

<c>

Figure 1 – 3: Method of surface charge modulation.

a. pH effect for surface charge density of nanochannel. [14]

b. Optoelectronic effect in solid state nanopore. [16]

c. Schematic diagram of a nanofluidic diode consisting of avidin patterned in half the channel. The other half has biotinmoieties, which result in a close to neutral surface charge and fluorescence image. The ionic currents were different with different surface treatment. [15]

`

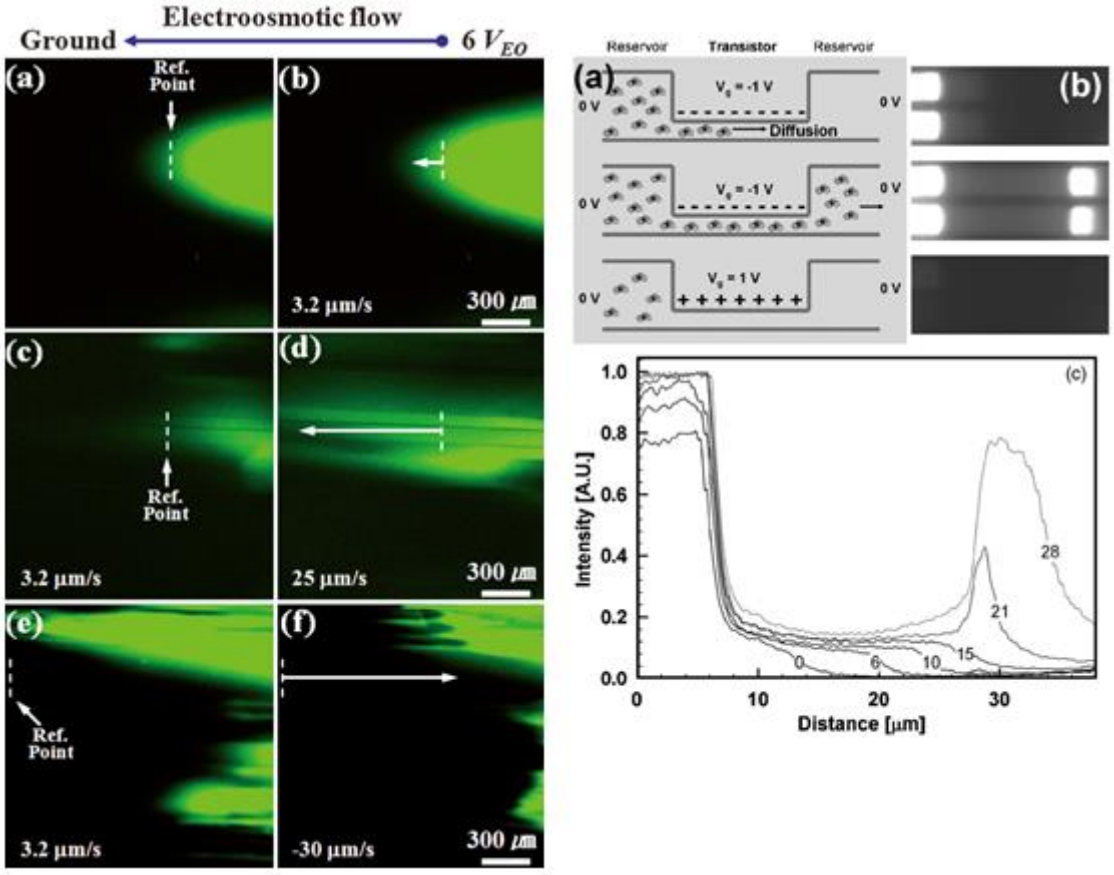

<a> <b>

Figure 1 – 4: Modified IFET (Ionic Field Effect Transistor).

a. Fluorescence images for floating gate, V_G = -30V – The dye flow accelerated; V_G = +30V – The dye flow in the reverse direction compared with floating and < - > gate voltage. Ambipolar behavior could control fluidic flow, accelerate and decelerate charged species dispersed in fluids additionally.

b. The avidin would transfer from left to right chamber, when the transistor was turned on (opposite polarity with avidin) without bias between the microchannels. And Fluorescence intensities were corresponding to amount of avidin flows. Ambipolar behavior could act as switch for charged species, so manipulate any charged species regardless of polarity.

`

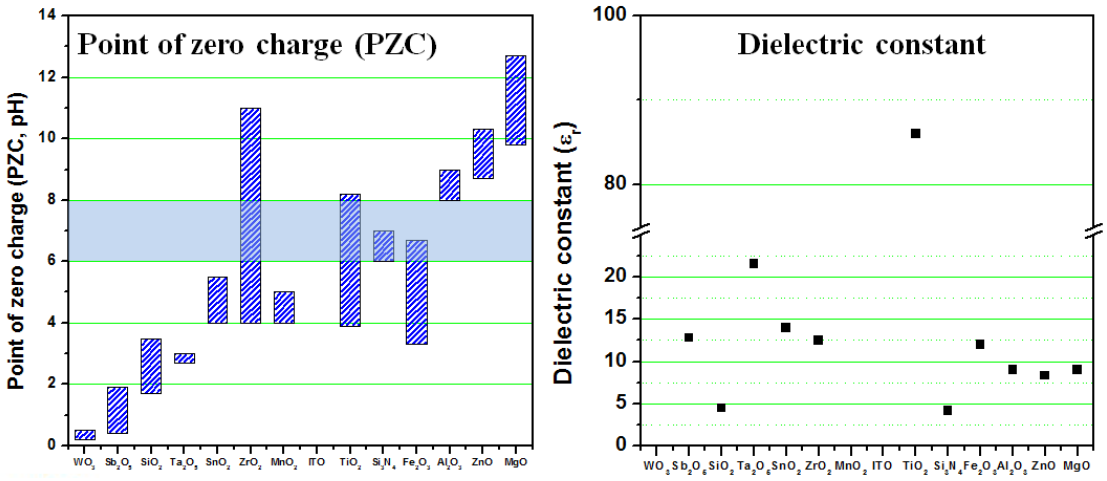

Figure 1 – 5: Investigate point of zero charge and dielectric constant of conventional oxide.

Consider the above two properties of material and possibility of deposition in our laboratory, we chose Al_2O_3 instead of SiO_2. Point of zero charge of Al_2O_3 is almost at pH 7, and dielectric constant is 2 times higher than SiO_2.

`

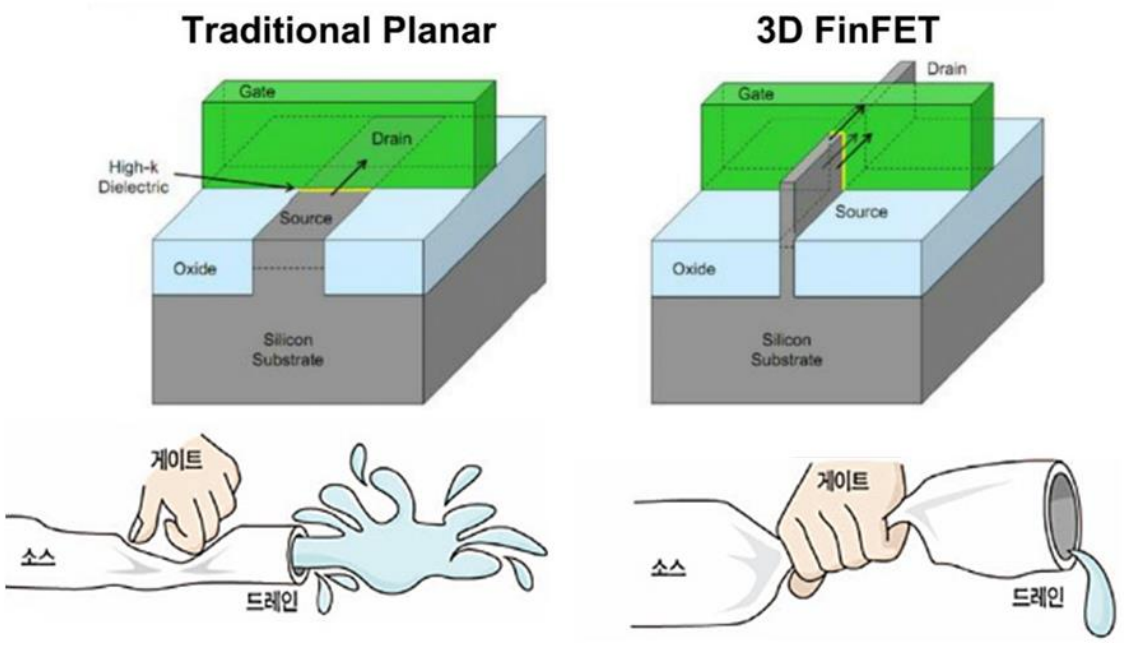

Figure 1 – 6: Schematic image of 3D FinFET structure in solid state electronic devices.

Capacitance of oxide is not only dependent with gate oxide material, but also related to gate structure. The image explained the gate structure effect vividly.

`

Chapter 2. Traditional numerical analysis about nanofluidic devices

`

2. Traditional numerical analysis about nanofluidic devices

1. Introduction

In order to intensively understand the transport phenomena in nanofluidic devices, we must comprehend the analytic numerical model and the physical meaning of the number from the model. And the reason of investigate nanofluidic system, it acts as a platform which can detect electrical signal or signal variation from charged species like ions, nanoparticles, and charged bio – molecules such as DNA, RNA, or protein transferring or its variation through the nanofluidic system, even a molecular level of variation. And all of these phenomena are completely governed by surface charge of nanofludic systems.

Within numerical model, fluid flow in the nanofluidic system are tightly coupled with chemical diffusion, drift by external electrical potential etc. each other. Therefore, Poisson's equation, Nernst-Planck equation and Navier-Stockes equation should be solved concurrently.

2. EDL (Electric Double Layer) theory

When immerse the solid into electrolyte, surface charge formation on the solid / liquid interface is formed, because of hydrolyzed reaction between solid / liquid interface. Depending on the equilibrium between ionized surface group and electrolyte, the solid will have either positive charged or negative charged. In order to maintain the electro neutrality at solid / liquid interface, the oppositely charged counter ions are will be attracted to the solid / liquid interface by electrostatic force, while the co – ions are repelled simultaneously. And this screening layer is named by EDL (Electric Double Layer) because it consists of counter ions ideally, and some of which are bound while left ones are mobile. Therefore, this interfacial layer constitutes a well – defined capacitor, and the thickness of layer will determine the capacitance.

Depending on ionic concentration, this layer has a thickness of from few nanometers to hundreds nanometers range. When systems have a large surface to volume ration or the physical

`

dimension are comparable to EDL (Electric Double Layer) thickness, the EDL (Electric Double Layer) plays an extremely roles in the system such our mentioned nanofluidic system.

With some assumptions, Gouy and Chapman developed a model. First, ions in electrolyte are treated as point charge, and do not interact each other. Second, fluid is linear isotropic homogenous material. Third, in the bulk potential are 0 and both the positive and negative ions have same concentration C_0, same as bulk concentration.

According to Gouy and Chapman model, at vicinity of charged surface, the model considered the thermal motion of ions; hence the ion should follow the Boltzmann distribution [Equation 1], and the surface potential should be the driving force to form the distribution, and that the surface potential was explained by Poisson equation [Equation 2]. They combined two equations into new one equation is called Poisson – Boltzmann equation (PBE) to numerically approach the model.

$n_i = {n_i}^{\infty} \exp(\frac{q(=z_i e)\varphi}{k_B T})$ – Equation 1 [1]

$\nabla^2 = \frac{d^2\varphi}{dx^2} = -\frac{\rho}{\varepsilon_r \varepsilon_0},\ \rho = e\sum_i n_i z_i$ – Equation 2 [1]

n_i is the ionic number concentration of the i[th] ionic species at the state, ${n_i}^{\infty}$ is the ionic number concentration at the neutral state where φ=0, z_i is the ionic valence of the i[th] ionic species, φ is electric potential of the surface, ρ is volume charge density of all ions present in the neighborhood of the surface, k_B and T are Boltzmann constant and temperature.

Because Boltzmann distribution is method of describing the probability of states also, in this region of distribution, the counter ions are predominant presented in, and the co – ions are not completely excluded, it is contrary with Helmholtz model which is constituted of counter ions only. And they dominated specific region as a diffuse (Gouy – Chapman) layer.

The diffuse layer thickness can express as characteristic length and obtain from the Poisson –

`

Boltzmann equation (PBE), denoted as λ_D [Equation 3]. The typical symmetric (z:z, z = 1) electrolyte solution at 25°C is illustrated Table. 2 – 1.

$$\lambda_D = \sqrt{\frac{k_B T \varepsilon_r \varepsilon_0}{2 z_i^2 e^2 n_i^\infty}}$$ – Equation 3 [1]

KCl concentration (M)	Debye length λ_D (nm)
10^0	0.3
10^{-1}	1.0
10^{-2}	3.1
10^{-3}	9.6
10^{-4}	30.5
10^{-5}	96.3

Table 2 – 1: Debye screening layer thickness at at 25°C (for typical symmetric (z:z, z = 1) electrolyte solution) [1]

Stern combined the Helmholtz model and Gouy and Chapman model into what is referred to as the classical EDL (Electric Double Layer) theory. He suggested that some ions adhered to the surface based on Helmholtz model, forming a stern layer, and left ones formed a diffuse layer. The Stern layer accounted for ions' finite size and consequently ions' closest approach to the surface is on the order of the ionic radius (few nanometers). In the stern layer, the ions absorbed by the surface are immobile, only the ions in the diffuse layer can contribute the ionic transport. An imaginary plane separates ions that immobile at the surface from those that are mobile in solution, which was referred as slip plane, and the potential at this plane was denoted as zeta potential (ξ – potential). [Figure 2 – 1]

Fail to explain highly charge surface is the biggest drawback.

3. Nernst – Planck equation and Navier – Stockes equation

The Nernst – Planck equation is a conservation of mass equation used to describe the motion of

`

chemical species in a fluid medium. Therefore, total ion flux in nanochannels can be assessed by Nernst – Planck equation [Equation 4]. And the equation is contributed by three terms: diffusion by concentration gradient, ion drift driven by electric field, and the last one is convection flow.

$\vec{J_i} = -D_i \left(\frac{z_i n_i e}{k_B T} \nabla\varphi + \nabla n_i\right) + n_i \vec{u}$ – Equation 4 [2]

J_i is the total flux in nanochannel, D_i is the diffusivity of ion, $\vec{u}$ is the velocity of fluid. Other notation is same as above-mentioned parts.

The Navier – Stockes equation describes the motion of fluid substance [Equation 5]. These equations arise from continuity equation for mass and momentum, and apply Newton's second law to fluid motion, together with pressure term, shear stress because of fluid viscosity, and external body force such as gravity, electrical force. In the case of nanofluidic system, the gravity is negligible and the electrical potential is dominantly effect the system. Furthermore, in nanofluidic system, with following condition for incompressible, laminar flow at steady state, we can simplify the Navier – Stockes equation with following equation. [Equation 6]

$-\nabla p + \eta \nabla \vec{u}^2 - \rho \nabla \varphi = 0$ – Equation 5 [2]

$\eta \nabla \vec{u}^2 - \rho \nabla \varphi = 0$ – Equation 6 [2]

p is the pressure of nanochannel system, η is the viscosity of fluid. Other notation is same as above-mentioned parts.

`

4. Reference

[1]. Reto B. Schoch et al., Rev. Mod. Phys., **80**, 839 – 883, (2008).

[2]. G. Pardon et al, Advances in Colloid and Interface Science, **199–200**, 78–94, (2013).

`

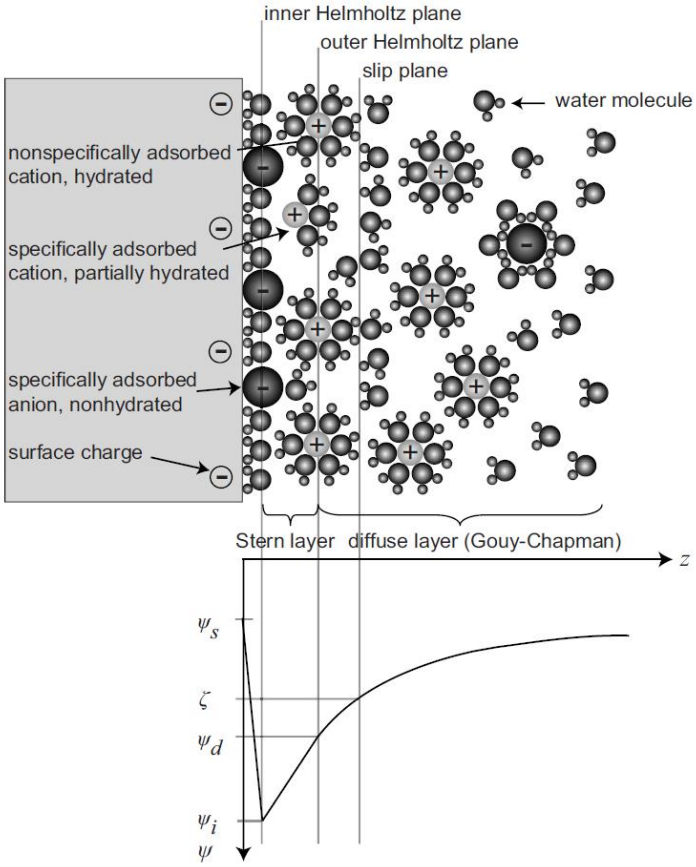

Figure 2 – 1: Scheme of EDL (Electric Double Layer) theory.

Gouy-Chapman-Stern models of the solid-electrolyte interface, with the corresponding potential distribution ψ vs the distance z from the wall. The inner Helmholtz plane layer (ψ_i) consists of nonhydrated co-ions and counterions, whereas the outer Helmholtz plane layer (ψ_d) is built up of only hydrated counterions. The diffuse layer is defined beyond the outer Helmholtz plane. At the slip plane, the ζ potential can be experimentally investigated, and it is usually equal to ψ_d.

`

Chapter 3. Detail fabrication process of nanochannel devices and measurement

`

3. Detail fabrication process of nanochannel devices and measurement

1. Introduction

In this chapter, I will demonstrate the detail fabrication method step by step. In comparison with vertical nanopore, lateral type nanochannel is more suitable for LOC (Lab – on – a – chip) device. And LOC device is subset of MEMS device so we used the fabrication method of MEMS industry, for instance, photolithography, RIE (Reactive Ion Etching), chemical wet etching etc. The lateral nanochannel devices have sufficient possibility of development at nanofluidc system for molecular logic circuit [1] and DNA sequencing [2] because of integration scheme.

So far, the presented all – around IFET (Ion field Effect Transistor) [1, 3-5] are more focused on the nanopore devices than nanochannel, because of common use of fabrication method of nanopore devieces. Sandwich type membrance (dielectric layer – patterned gate electrode layer – dielectric layer) replays the typical dielectric membrane of solid state nanopore. And the membrane is drilled by FIB (Focused Ion Beam) method owing to the typical electron beam form TEM cannot penetrate the thicker sandwich type membrane. Although the FIB (Focused Ion Beam) drilled nanopores have relatively large diameter, can reduce the pore with ALD (Atomic Layer Deposition) method to compare with TEM drilled nanopore.

2. Wafer preparation

Nanochannel fabrication started with 500 μm P – type Si (100) wafer. At first, SiO_2 1μm was deposited by PECVD (Plasma Enhanced Chemical Vapor Deposition) with TEOS (tetraethyl orthosilicate) precursor and α – Si 25 nm was deposited by LPCVD (Low Pressure Chemical Vapor Deposition), sequentially. [Fig 3 – 1]

`

3. Part of nanochannel fabrication

Figure 3 – 2 shows the overall procedures for fabrication of naochannel parts. Using electron beam lithography (EBL) to define the primary line structure of nanochannels, the poly methyl methacrylate (PMMA) was used as E – beam resistor. And developed the E – beam patterning with developer, 80 arrays nanotrenches on PMMA with size of 50 μm length and 140 nm wide was obtained. Two – steps Reactive Ion Etching (RIE) was carried out to transfer the nanotrenches from poly methyl methacrylate (PMMA) to prepared Si substrate.

The recipes of the two – steps RIE are as follows; First step – gas type and flow rate: SF_6 (35 sccm), O_2 (15 sccm), time: 30 s, pressure: 10 mTorr, power: 30 W rf; second step – gas type and flow rate: CHF_3 (25 sccm), Ar (25 sccm), time: 400 s, pressure: 30 mTorr, power: 100 W rf. The first step of RIE aimed to etch α – Si and subsequently, the second one purposed to open the SiO_2 layer. Then the patterned nanotrenches on PMMA perfectly transferred to prepare Si substrate with 140 nm widths, 100 nm depth and 50 μm lengths and the number of nanotrenches were 80. (Depth of nanotrench can be controlled by etching time and power.) And O_2 plasma was used to remove the PMMA residue. Figure 3 – 3 shows the SEM cross section image for nanotrenches. α – Si and SiO_2 have good wet etching selectivity in chemical like DHF (Dilute Hydro fluoric Acid) or BOE (Buffered Oxide Etchant). The etching rate of DHF was less stable than BOE with time. Thus, we chose the BOE for wet etchant and the etch rate of dilute BOE is 0.4 nm/s. For obtained the final channel with ~ 10nm diameter, we etched 20 s in dilute BOE. [Figure 3 – 4] As result, because of the characteristics of isotropic etching of wet etching, BOE etchant generated undercut of SiO_2 layer, and made the cross – section of nanotrenches as semicircular shape. As gate electrode, TCO (Transparent Conduct Oxide) of AZO (Aluminum doped Zinc Oxide) was deposited 35 nm (9 set cycles, ZnO : Al_2O_3 = 24 : 1) on the whole surface of devices by ALD (Atomic Layer Deposition). We could observe the detail information for etching and AZO (Aluminum doped Zinc Oxide) deposition with SEM image. [Figure 3 – 5]

`

Compare to opaque metal electrode, we can electrically tuning the charged species in nanochannels, and also optically observe the movement changes of charged species, and this is the biggest merit of the device. We deposited TCO (Transparent Conduct Oxide) of AZO (Aluminum doped Zinc Oxide) on the whole surface of devices, and the nanochannels was buried in the Si substrate totally, therefore, when we open the nanochannels, the gate electrode make unwanted electrical path of device. In order to close off the unnecessary path of circuit, we patterned the gate electrode, removed AZO at the edge of nanochannels with dilute HNO_3 (1000 : 1), and just remained the 10 μm of gate electrode at the center of nanochannels. [Figure 3 – 6] The material of gate electrode – TCO (Transparent Conduct Oxide) of AZO (Aluminum doped Zinc Oxide) is mechanically weak, thus we only deposited copper electrode pad on the AZO contact area with measurement probe, using E – beam evaporator with hard mask. Then, depositing 70 nm Al_2O_3 (0.12 nm / cycle × 584 cycles)as dielectric layer of FET structure also by ALD (Atomic Layer deposition) process that pipe structure nanochannels with all – around partially gated (only at the center of nanochannels) was formed. [Figure 3 – 7], [Figure 3 – 8] We illustrated schematic image of nanochannels to comprehend structure of nanochannels easily. [Figure 3 – 9]

Because the ALD (Atomic Layer deposition) process is most conformable deposition method, [Figure 3 – 10], [6] the deposition can obtain on undercut 3 – D structure. And the owing to the undercut structure, regardless of the nanotrenches size, the final pipe structure nanochannels size will be determined by undercut length (degree of wet etching).

4. Microchannel formation and nanochannel opening

For the purpose of forming microchannel, we deposited 1.5 μm thickness of SiO_2 on the entire device covered by Al_2O_3, using PECVD (Plasma Enhanced Chemical Vapor Deposition). Hereafter, we used photo lithography method to pattern microchannel and used RIE (Reactive Ion Etching) process for two steps to form the microchannel was connected with nanochannels;

`

first step – gas type and flow rate: CHF_3 (25 sccm), Ar (25 sccm), time: 40 min with 1 hour break time each of 10 mins, pressure: 30 mTorr, power: 200 W rf; second step – gas type and flow rate: Ar (50 sccm), time: 20 min with 1 hour break time each of 10 mins, pressure: 100 mTorr, power: 200 W rf. The first step of RIE aimed to etch SiO_2 layer deposited by PECVD (Plasma Enhanced Chemical Vapor Deposition) and the second one is used to etch Al_2O_3 layer. Because we do not possess the RIE (Reactive Ion Etching) of Al_2O_3, Ar physical sputtering method was used for Al_2O_3 layer. When patterning the microchannel, we set the gap of two microchannels of both side of nanochannels for 20 μm so that the entire system of nanochannels was 20 μm of total length and 10 μm gate embedded at center of the nanochannels. And the microchannel had dimensions as follows: 100 μm wide, 1.5 μm depth [Figure 3 – 11]. We also implanted three pillars with 10 μm diameter to avoid flexible PDMS (Polydimethylsiloxane) collapse. Finally, using PDMS cover bonded to device with O_2 plasma with condition of O_2: 100 sccm, 50 mTorr, 10 W, 30 s, and heated at 95 ^oC by hot plate. With this, all fabrication process had finished. [Figure 3 – 12]

5. Measurement method

Existing IFET (Ionic Field Effect transistor) have worked at lower concentration electrolyte (KCl solution) from 10^{-5} to 10^{-2} M. [7 – 10] Due to the the Debye layer thickness (λ_D) of lower concentration is comparable to nanochannel thickness. The same as existing results of other group researches, we measured the ionic current (I_D) not only from 10^{-5} to 10^{-2} M, also measured at 10^{-1} and 1 M of more harsh conditions.

At low electrolyte concentration from 10^{-5} to 10^{-2} M, we didn't find other differences. However, we found the special phenomena that have never seen before; it is precipitation of the crystal KCl in the microchannel [Figure 3 – 13]. The solubility of KCl in water is 360 g / 1 kg of water at 25^oC [11], if we converse the unit, that number is equal to 5 M (360 g / 1 kg = 5 M). In other words, our device acted as preconcentor, and preconcentrated at least 50 times.

`

And Ko *at al* report the <Nanofluidic preconcentration device in a straight microchannel using ion concentration polarization>, which demonstrates nanofluidics device possible to enhance the strength of ionic concentration more than 500 folds than before [13], therefore, the phenomena of precipitation is reliable in our system. However, with careful observation during measurement, the precipitation of crystal KCl is not only occurred at interface between microchannel and nanochannel [12 – 13], also be found in the microchannel. We thought the precipitation cause of limitation of fabrication method. Microchannel walls are made of SiO_2, and height of channel is only about 1 μm. Coupled with PDMS (Polydimethylsiloxane) cover flapped down, the height of microchannel will be insufficient miro – size, so the microchannel acts as nanochannel nealy. The typical value of surface charge of SiO_2 is ~-50 mC/m^2,[14] it will promote the precipitation phenomena. Therefore, for high concentration electrolyte like 10^{-1} and 1 M, we flushed the microchannel after each measurement to prohibit precipitation. Current method is not practical for high electrolyte concentration like 10^{-1} and 1 M.

To make sure the reliability of gate electrode, we swept voltage between two metal electrode tap on the gate electrode. The sweeping voltage from 1V to -1V, and back to 1V, and the measurement results shows in Figure 3 – 14 (10^{-5} level). The gate electrode AZO (Alumium doped Zinc Oxide) exhibit electro resistivity of $10^{-3}\Omega cm$, deposited by our group ALD equipment [15]. And consider structure of the electrode (W × H × L = μm × nm × cm), this theoretical value well matched with the experimental. After confirm the reliability of the gate electrode, Ag / AgCl electrode in *trans* and *cis* reservoir diagonal direction was connected to drain and source probes, respectively, and lifted up one probe that was connected with gate electrode of device. So we connected the total electrical circuit, as shown in Figure 3 – 15. For prove our device has more sensitive than existing devices and effectively measure, we decided voltage level of V_{SD} (Source – Drain Voltage) and V_G (Gate Voltage) as follow, V_{SD} = -2 ~ 2 V with interval of 0.5V and V_G = -2 ~ 2 V with interval of 0.5 V, too. IFET (Ionic Field Effect transistor) exhibits ohmic behavior with variation of Source – Drain Voltage at below -5 or 5 V,

`

but increase the voltage more than this level, Nonlinear I_{SD} vs V_{SD} characteristic have been observed. [1, 6]. The electron mobility in Si device (1500 $cm^2/V \cdot S$) is 7 orders greater than ionic mobility in electrolyte (K^+: 7.616 x 10^{-4} $cm^2/V \cdot s$, Cl^-: 7.909 x 10^{-4} $cm^2/V \cdot s$), we should have sufficient time to stabilize current because of RC delay. Figure 3 – 16 shows the current stabilizing time at least 60 ~ 70 s for our device. For the same reason, we also need gate voltage enough rising time to maximize the gate effect.

As mentioned above paragraph, preconcentration and deconcentration phenomena at two interfaces between microchannel and nanochannel occurred by dc bias, and the direction of bias determined the direction of the preconcentration and deconcentration region, and vice versa. Owing to neutralize the concentration gradient, we also added 5 min of extra relaxation time when change the bias direction. Figure 3 – 17 shows the I_{SD} current when gate was floating, in the graph, the current value exhibits convergent tendency from the third measurement. Therefore, we chose the current value of third measurement as the float current.

`

6. Reference

[1]. Kee – Hyun Paik et al., ACS. Nano, **6**, 6767 – 6775 (2012).

[2]. Cess Dekker et al., Nature nanotech. **2**, 209 – 215 (2007).

[3]. Zhijun Jiang et al., Phys. Rev. E, **83**, 031203 (2011).

[4]. S. Nam et al., *Nano Lett.*, **9 (5)**, 2044–2048 (2009).

[5]. S. Nam et al., *Nano Lett.*, ***10*** **(9)**, 3324–3329 (2010).

[6]. Do-Joong Lee et al., J. Phys. Chem. C, **118**, 408−415 (2014).

[7]. Udi Vermesh et al., Nano Letter, **9 (4)**, 1315-1319 (2009).

[8]. Weihua guan et al., Nature Communications 2, Article number: 506 (2011).

[9]. Zhijun Jiang et al., Phys. Rev. E, 83, 031203 (2011).

[10].S. Nam et al., Nano Lett., 9 (5), 2044–2048 (2009).

[11].http://en.wikipedia.org/wiki/Solubility_table.

[12].Sung Jea Kim et al., PhysRevLett., 99, 044501 (2007).

[13].Sung Hee Ko et al., Lab Chip, 12, 4472–4482 (2012).

[14].Yuhui He et al., ACS Nano, 5 (7), 5509 – 5518 (2011).

[15].Do-Joong Lee et al,. Adv. Funct. Mater., 21, 448–455 (2011).

`

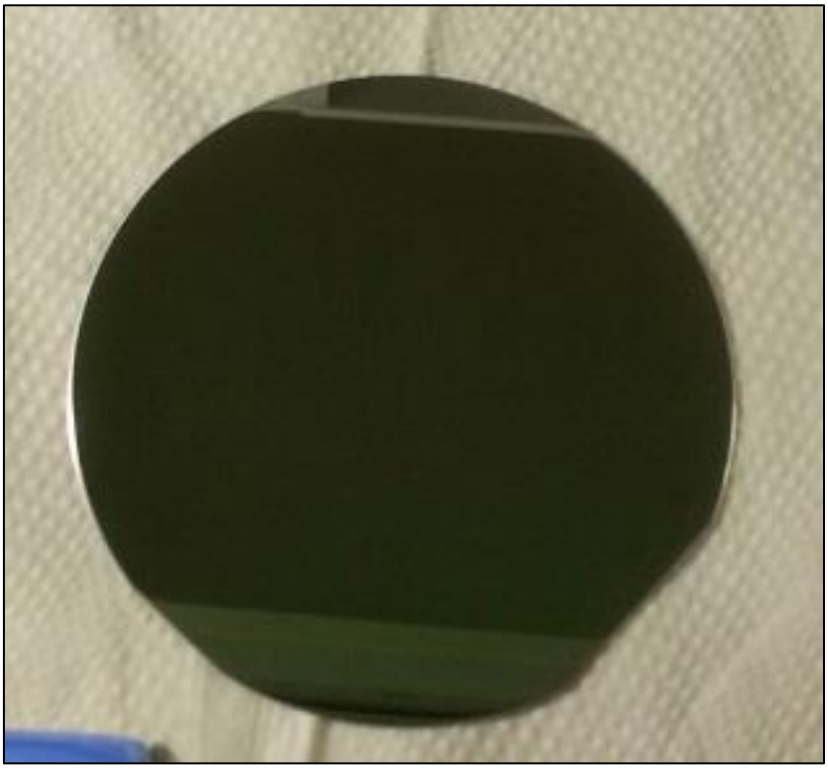

Figure 3 – 1: Prepared wafer with sandwich type (Si (100) wafer / SiO2 1μm / α – Si 25nm).

500 μm P – type Si (100) wafer + SiO2 1μm – PECVD (Plasma Enhanced Chemical Vapor Deposition) with TEOS (tetraethyl orthosilicate) precursor + α – Si 25 nm – LPCVD (Low Pressure Chemical Vapor Deposition.

`

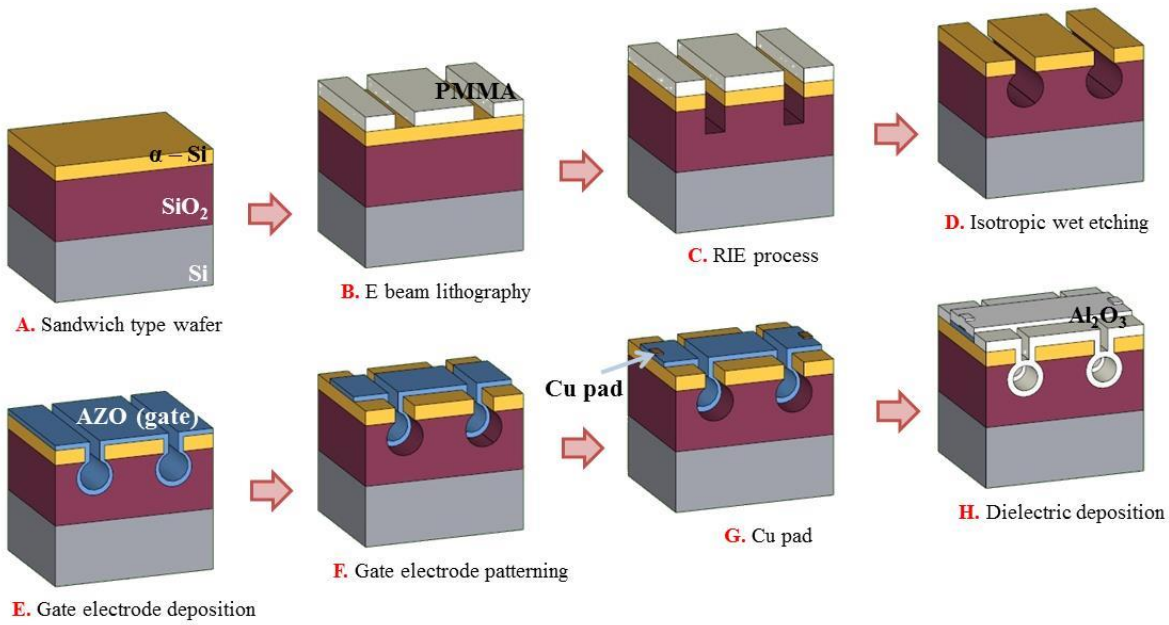

Figure 3 – 2: Overall procedures for fabrication of naochannel parts.

A. Sandwith type wafer preparation.

B. E – beam patterning with developer, 80 arrays nanotrenches on PMMA with size of 50 μm length and 140 nm wide.

C. First step: SF_6 (35 sccm), O_2 (15 sccm), time: 30 s, pressure: 10 mTorr, power: 30 W rf; second step: CHF_3 (25 sccm), Ar (25 sccm), time: 400 s, pressure: 30 mTorr, power: 100 W rf.

D. Dilute BOE wet etching 20 s with etching rate 0.4 nm/s.

E. TCO (Transparent Conduct Oxide) of AZO (Aluminum doped Zinc Oxide) was deposited 35 nm (9 set cycles, ZnO : Al_2O_3 = 24 : 1).

F. Removed AZO at the edge of nanochannels with dilute HNO_3 (1000:1).

G. Cu pad was deposited by E – beam evaporator, because AZO (Aluminum doped Zinc Oxide) is mechanically weak.

H. Depositing 70 nm Al_2O_3 (0.12 nm / cycle × 584 cycles)as dielectric layer of FET structure.

`

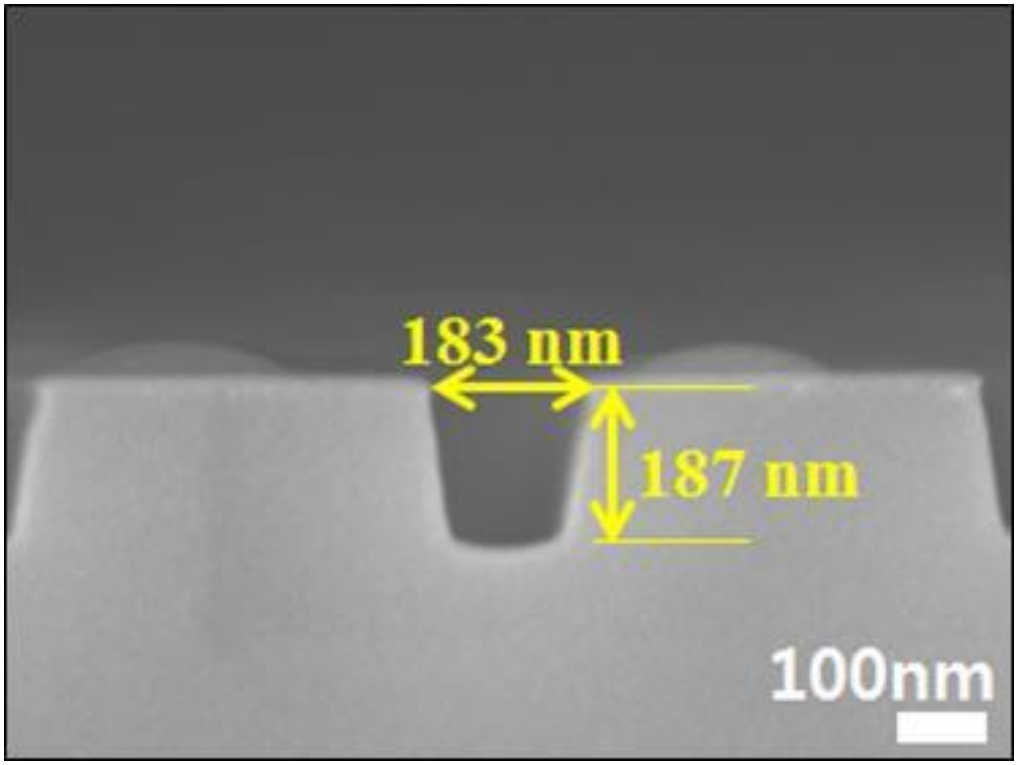

Figure 3 – 3: SEM cross section image for nanotrenches.

After two – steps of RIE (Reactive Ion Etching), size of nanotrenches will be 183 nm width × 183 nm heights. The size of nanotrenches from the SEM imag is well matched with the calculate size with etching rate. (25 ~ 28 nm/min at 200 W rf).

`

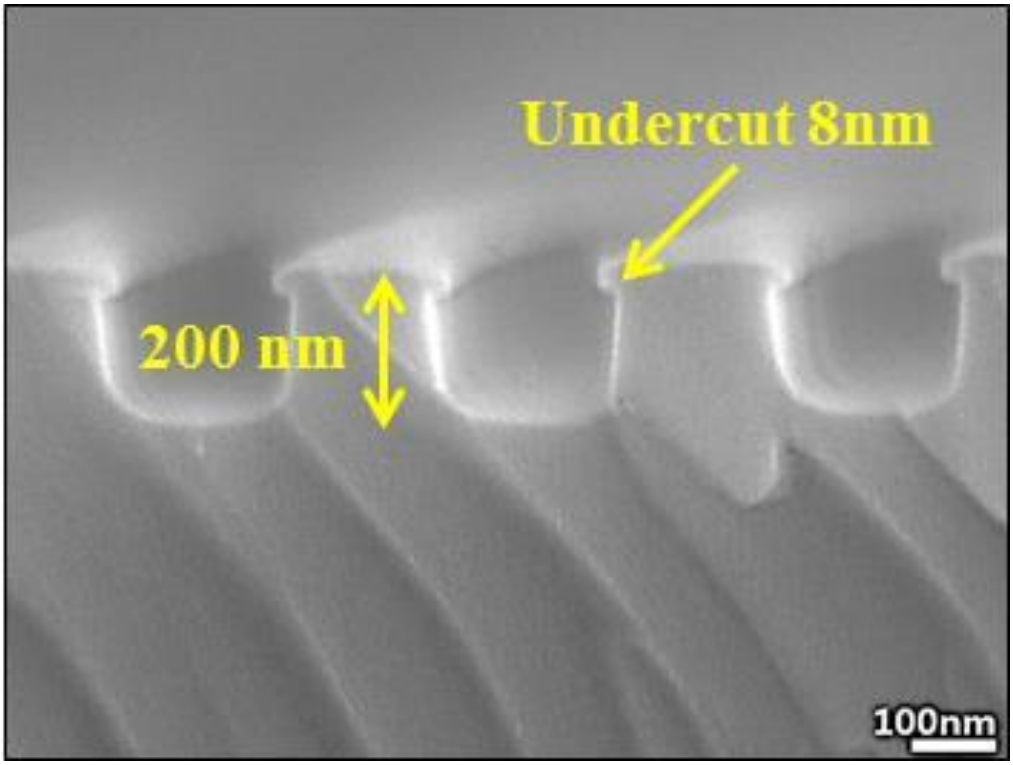

Figure 3 – 4: SEM image of after dilute BOE wet etching.

Wet etchant and the etch rate of dilute BOE is 0.4 nm/s. For obtained the final channel with ~ 10nm diameter, we etched 20 s in dilute BOE.

`

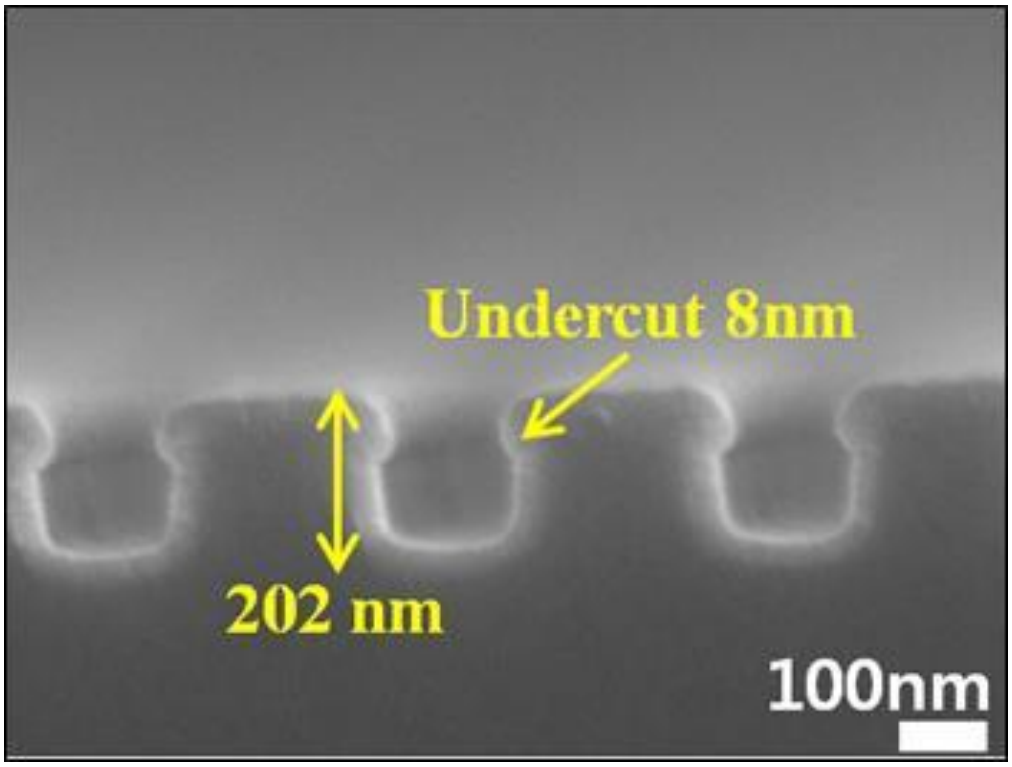

Figure 3 – 5: AZO (Aluminum doped Zinc Oxide) deposition with ALD.

As gate electrode, TCO (Transparent Conduct Oxide) of AZO (Aluminum doped Zinc Oxide) was deposited 35 nm (9 set cycles, ZnO : Al_2O_3 = 24 : 1).

`

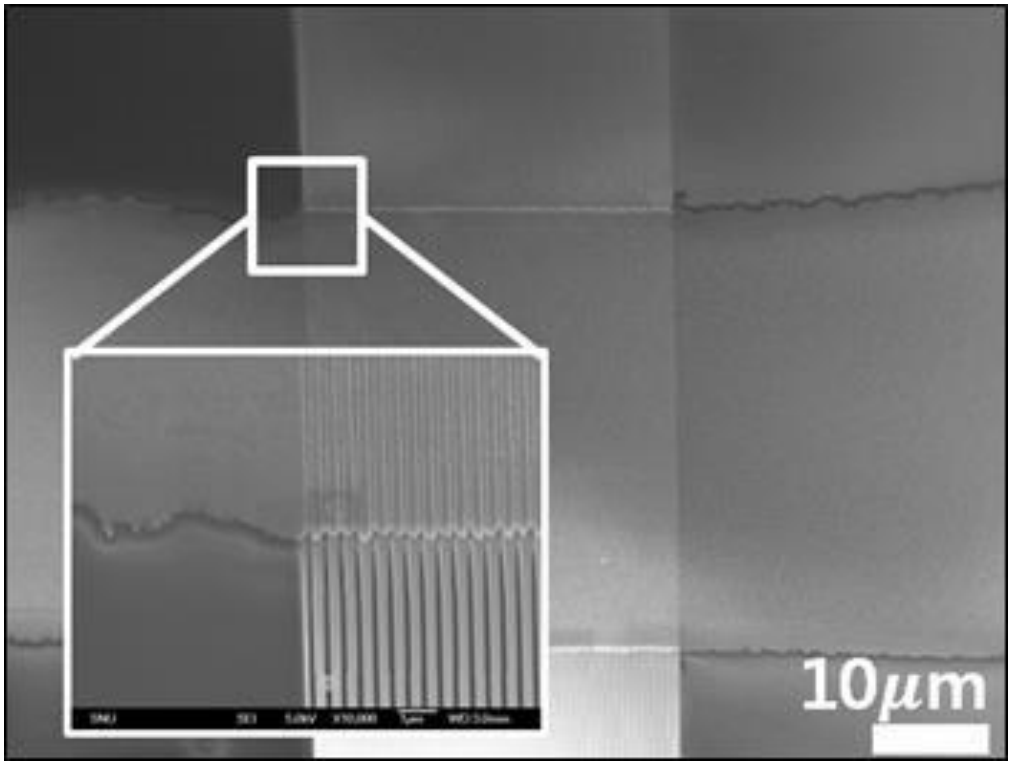

Figure 3 – 6: Removed AZO at the edge of nanochannels to prevent unwanted electrical path.

Patterning the gate electrode, removed AZO at the edge of nanochannels with dilute HNO_3 (1000:1), and just remained the 10 μm of gate electrode at the center of nanochannels.

`

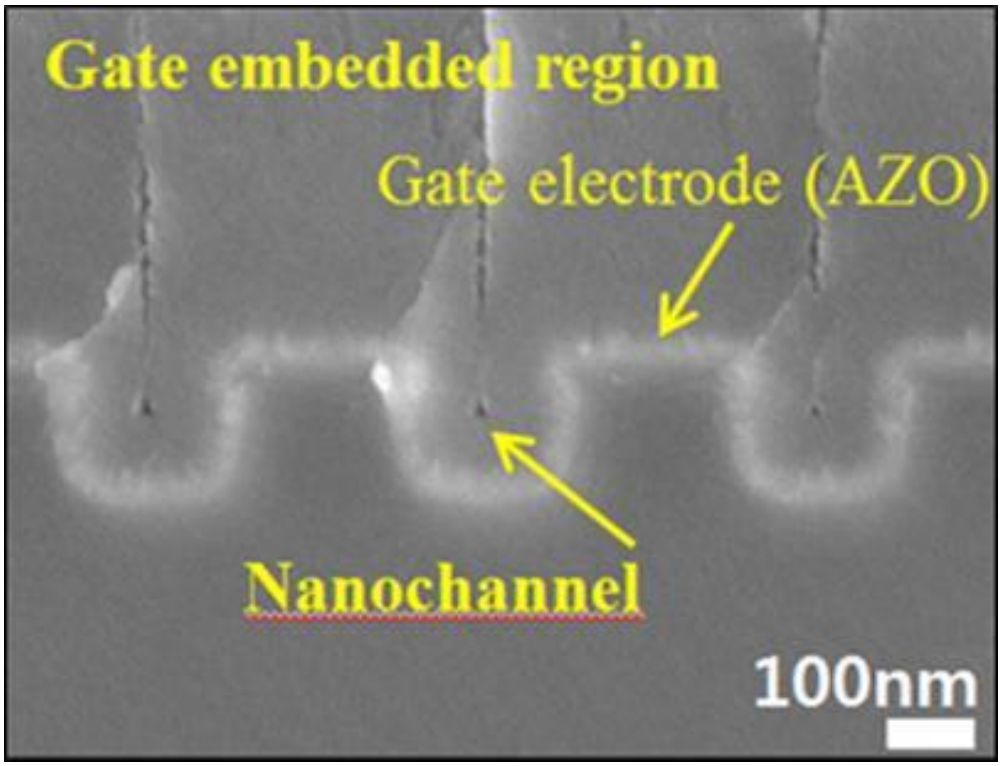

Figure 3 – 7: SEM cross section view of gate embedded region.

`

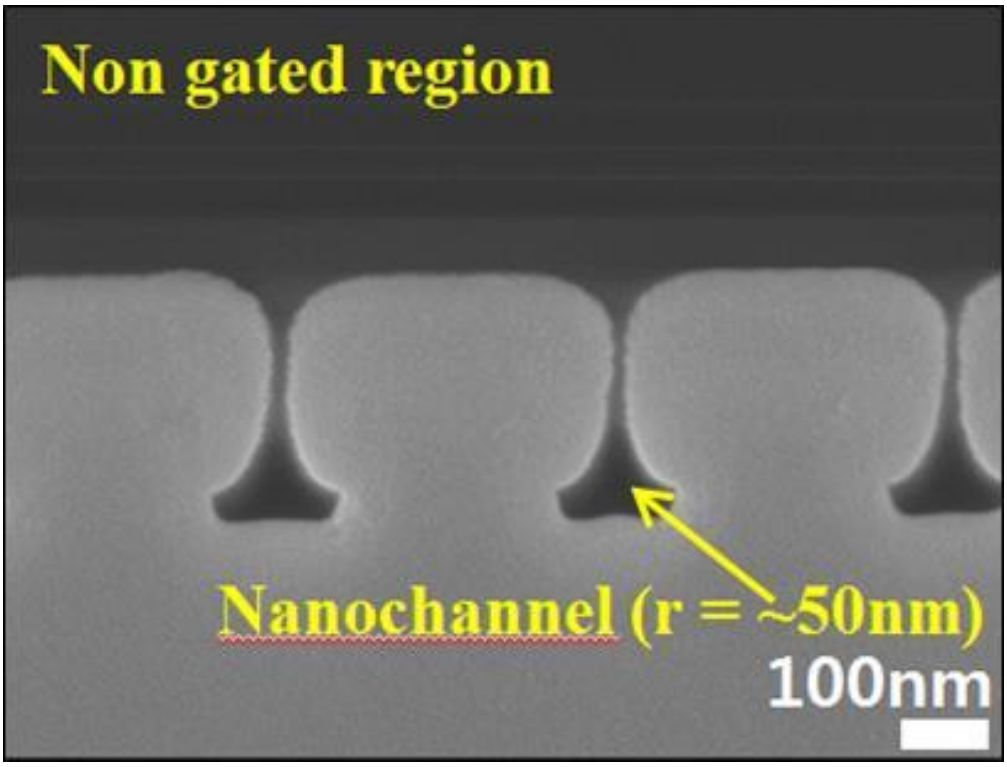

Figure 3 – 8: SEM cross section view of gate not embedded region.

`

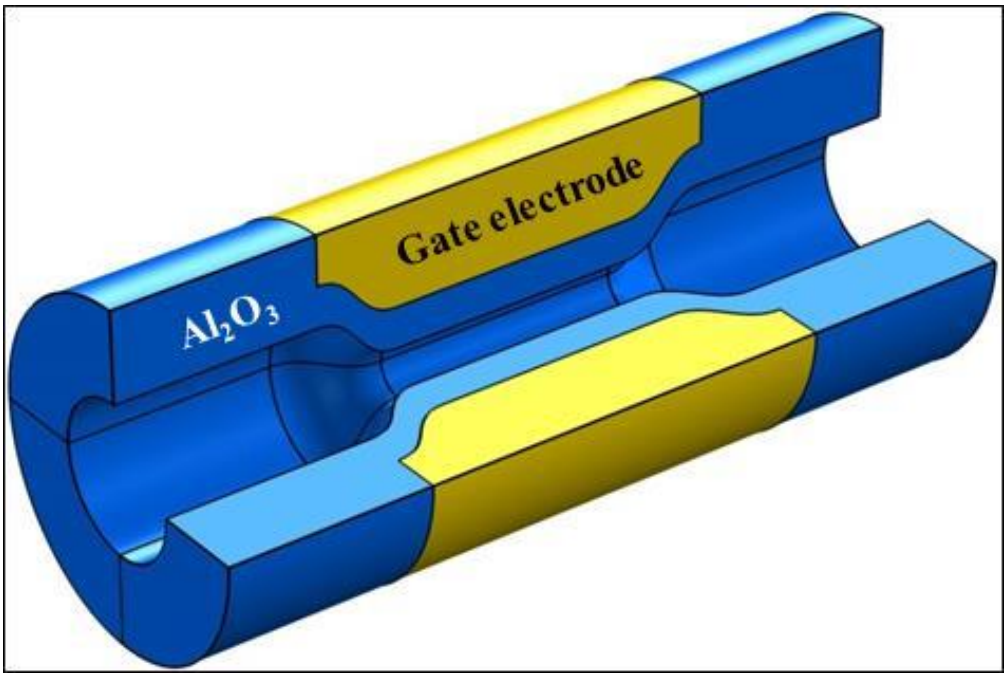

Figure 3 – 9: Schematic image of nanochannels part.

`

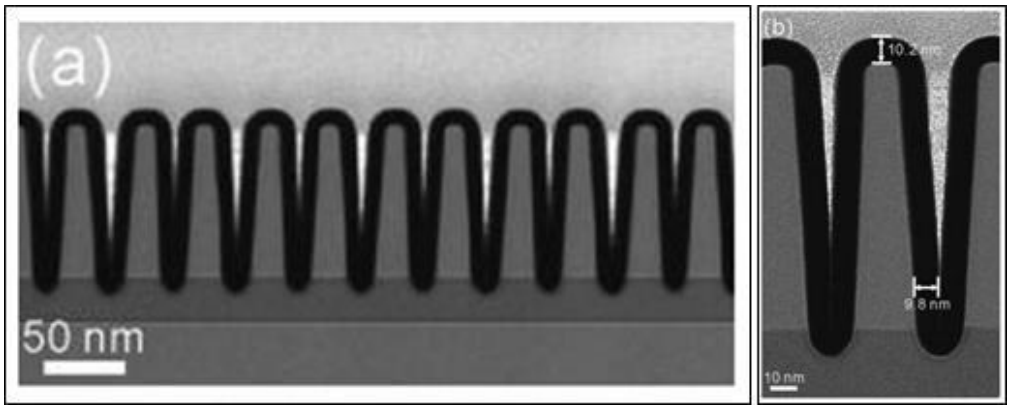

Figure 3 – 10: ALD deposition on the surface with high aspect ratio.

ALD is a deposiotin method with atomic scale, therfore ALD supply the most conformable film with any structure. [6]

`

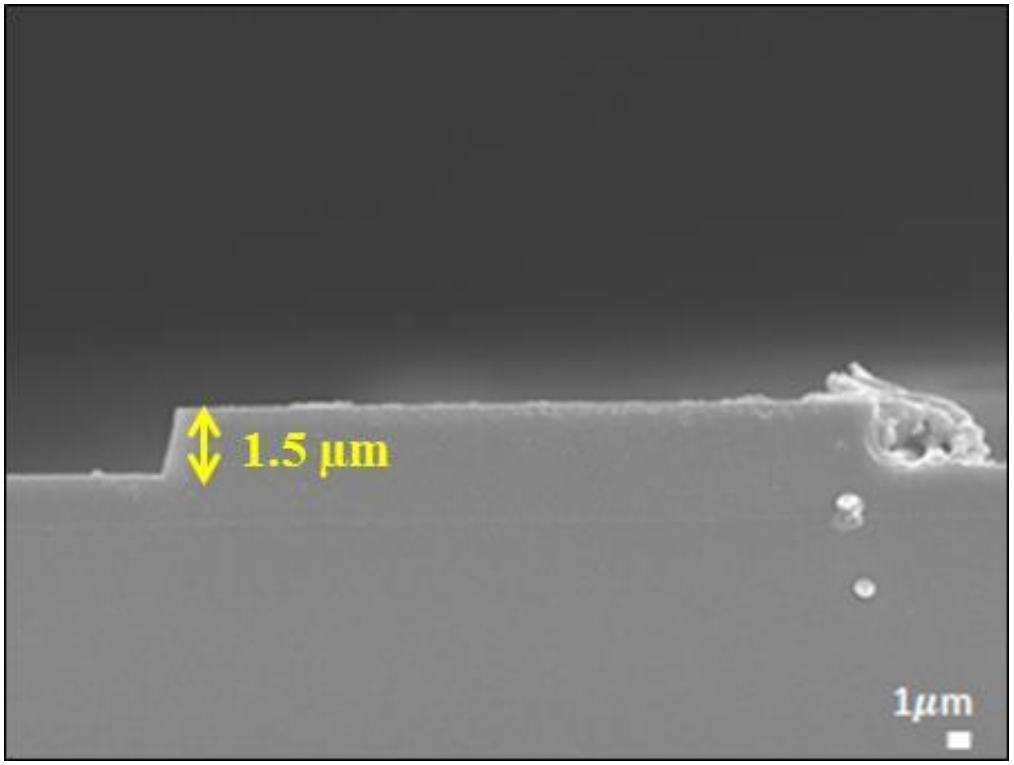

Figure 3 – 11: SEM cross section view of micro – pillar in microchannel.

Prevent PDMS collapse with microchannel, insert 1.5 µm heights micropillars in microchannel.

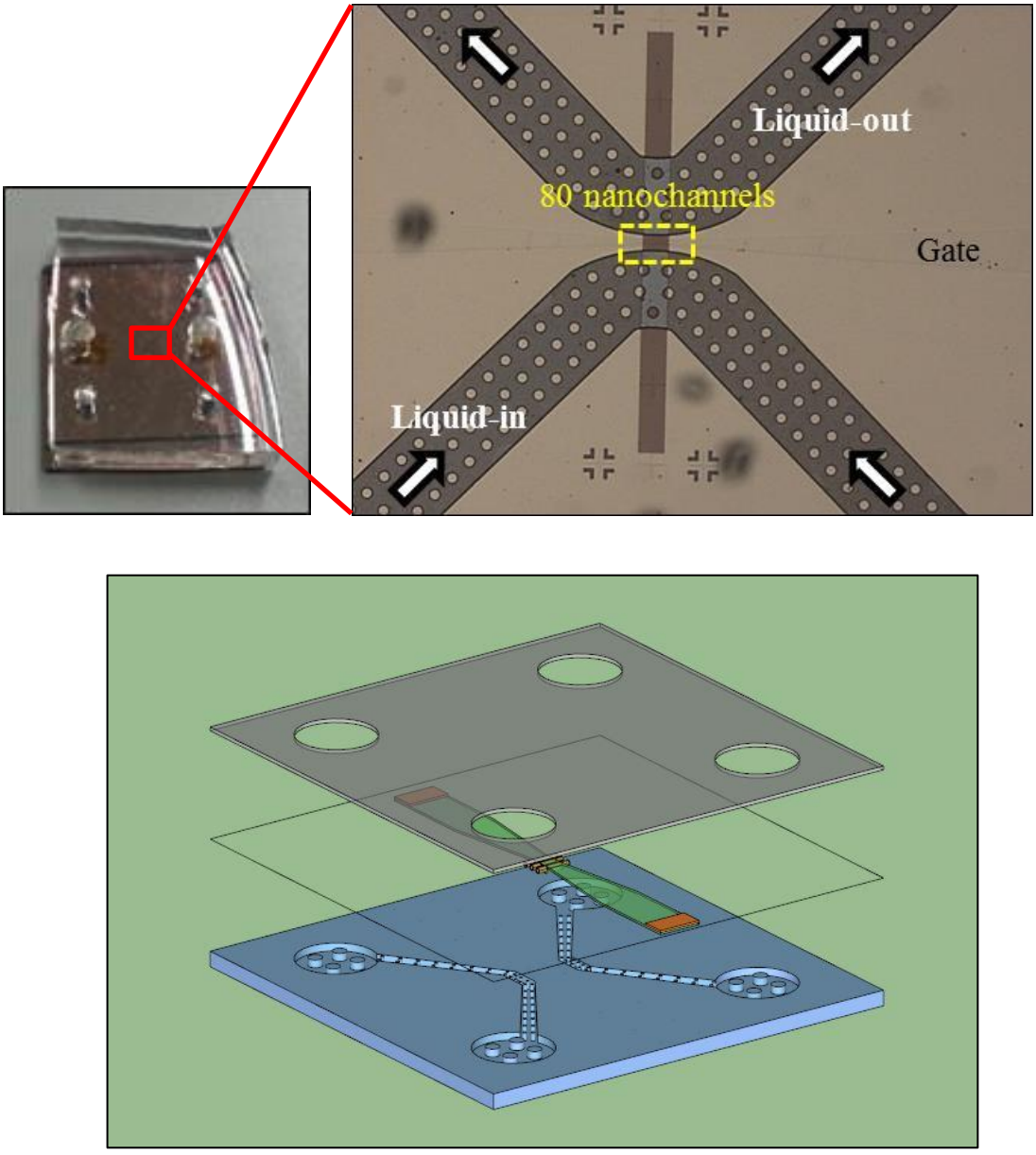

Figure 3 – 12: Optic image and explosion view of nanochannels devices.

`

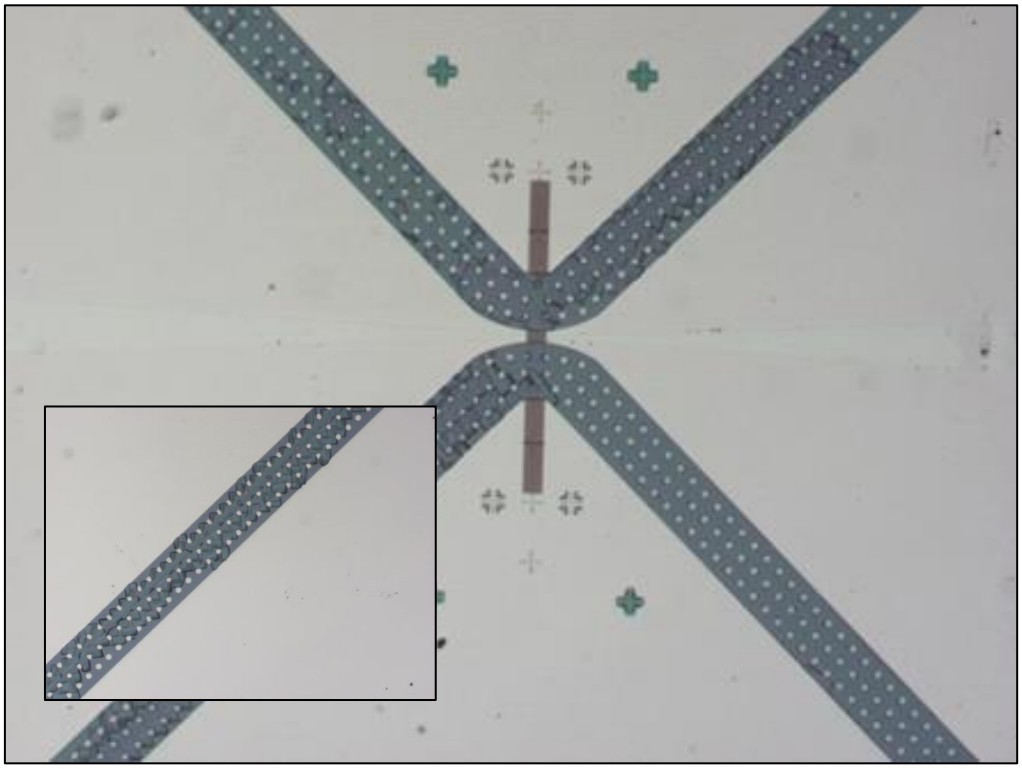

Figure 3 – 13: Optic image for precipitation in microchannels.

Precipitation of KCl crystal was found in microchannels. We though this phenomena may be a relationship with ICP (Ion Concentration Polarization).

`

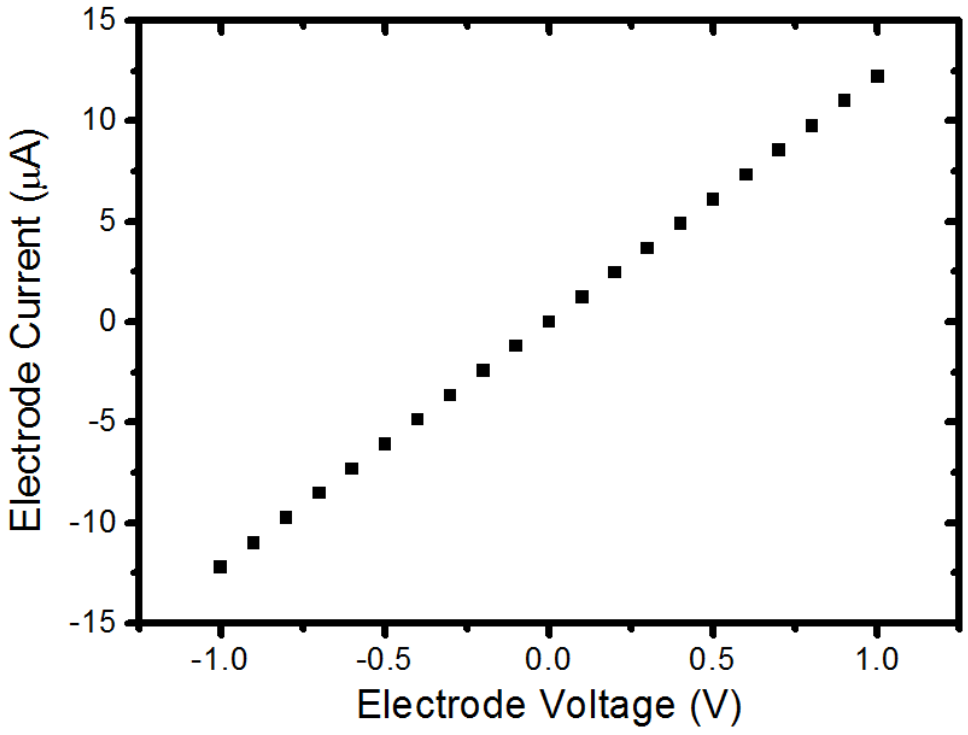

Figure 3 – 14: Gate electrode current, ρ of AZO $\approx \sim 10^{-3}\ \Omega \cdot$ cm. [9]

Electrode structure is (W × H × L = μm × nm × cm), and R = ρ x $\frac{l}{A}$ = ~ MΩ, so I = V/R = ~ μA.

`

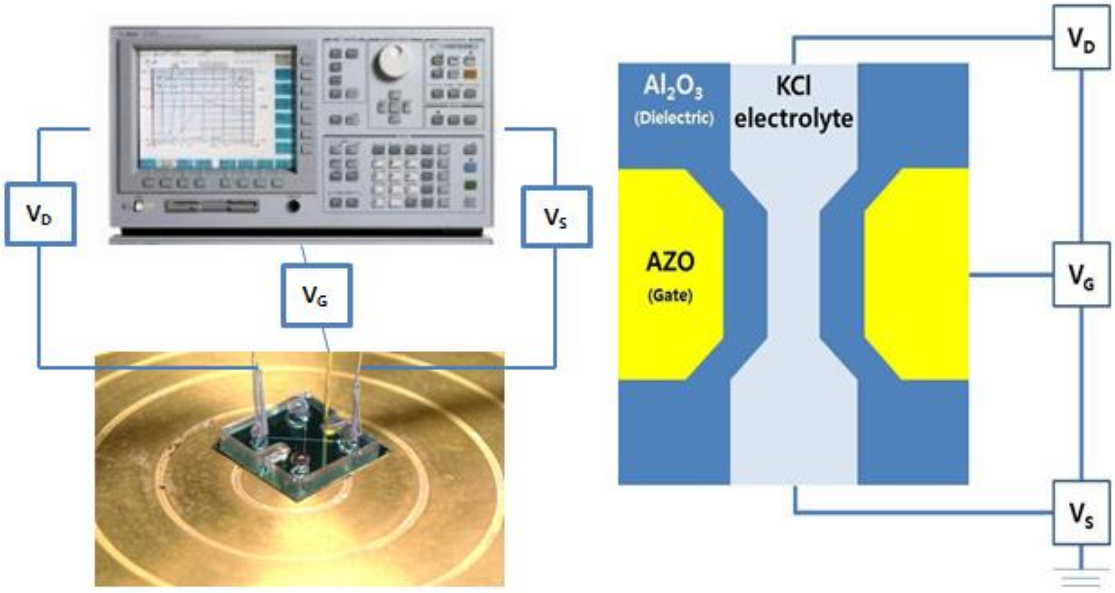

Figure 3 – 15: Schematic and optical image of electrical circuit.

Simultaneous measurement of currents is from drain voltage, gate voltage, and source voltage. Moreover, we could obtain the following conclusions: I_D (Drain current) = I_G (Gate current) + I_S (Source current). Therefore, the gate effect will be dominated by gate current (leakage current).

`

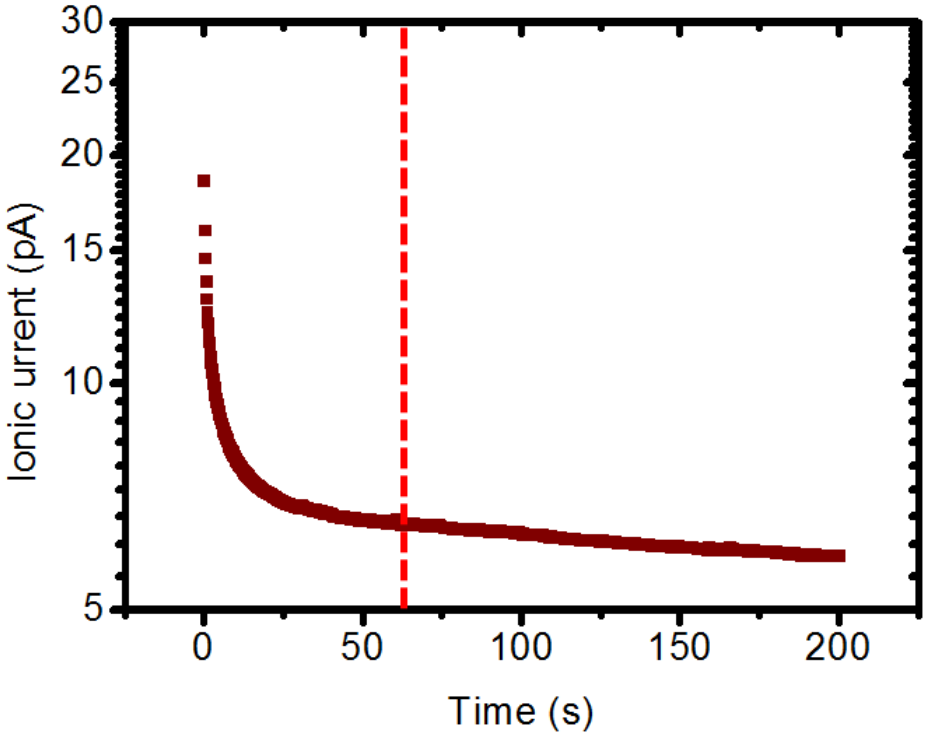

Figure 3 – 16: RC delay with nanochannels devices.

Because of ion mobility in electrolyte, our devices need 60 ~ 70 s RC delay time at least.

`

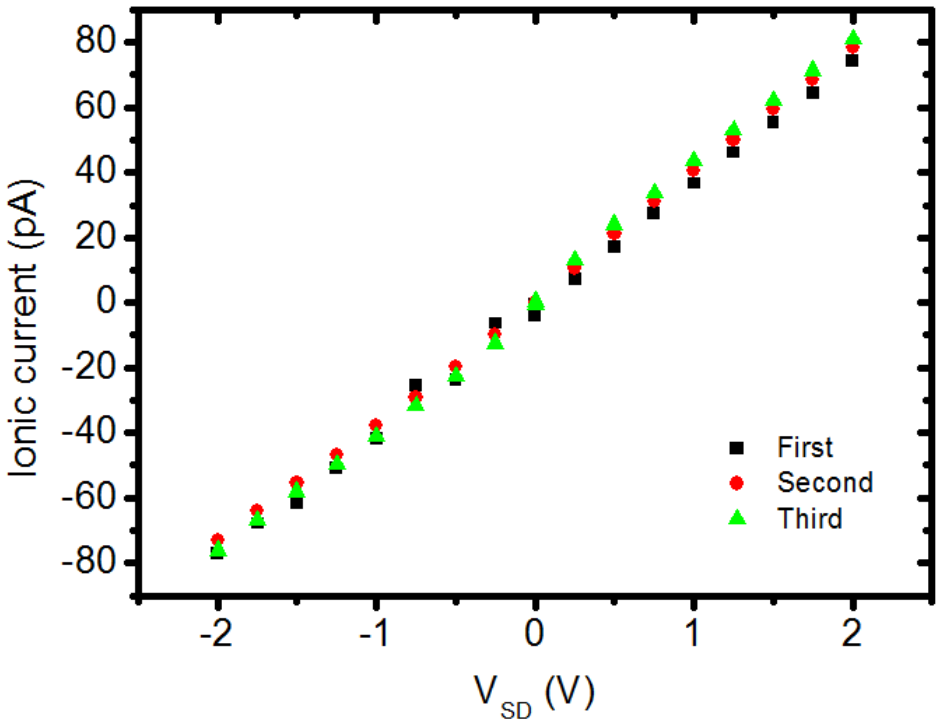

Figure 3 – 17: Floating current measurement with 3 times (at 10^{-5} M).

The first result of measurement is lowest. The second ones and the third ones are similar mostly.

(It has some difference case by case.)

`

Chapter 4. Result and discussion

`

4. Result and disscusion

1. Ionic current

We have mentioned the measurement procedure in previous chapter, and the detail measurement level of V_{SD} (Source – Drain Voltage) = -2 ~ 2 V with interval of 0.5 V, and V_G (Gate Voltage) was the same. Figure 4 – 1 shows the floating ionic current without gate voltage applied. The figure illustrated ionic current increase with bulk concentration increase; it is obvious because KCl concentration is the carrier concentration of the electrical circuit, and ionic current gave us ohmic behavior within range of V_{SD} (Source – Drain Voltage) = -2 ~ 2 V.

Regardless of gate voltage polarity, we were able to confirm the gate effect. Except for variation with gate voltage, other condition such as V_{SD} (Source – Drain Voltage), KCl concentration are fixed. We obtained the explicit difference between floating state and applying voltage to the gate voltage. And the delta ionic current is always positive relatively regardless of gate voltage polarity. Compare the Debye screening length with nanochannel dimension, at low KCl concentration regime about $10^{-5} \sim 10^{-4}$ M, the difference between the former and the latter is not pronounced, thus, the surface charge density will totally govern the ionic current. At results, there is no difference at low KCl concentration regime about $10^{-5} \sim 10^{-4}$ M. [Figure 4 – 2], [Figure 4 – 3] In the same view, at middle KCl concentration regime about $10^{-3} \sim 10^{-2}$ M, ionic currents was governed by bulk and surface property simultaneously. [Figure 4 – 4], [Figure 4 – 5] At higher KCl concentration, we found the phenomena of precipitation of KCl crystal in microchannel, and just suspected the precipitation phenomenon was caused by ICP (Ion Concentration Polarization). Moreover, we did not have sufficient evidence to prove it, therefore, it will be an interesting research topic for further study, and will focus on low and middle KCl concentration region from $10^{-5} \sim 10^{-2}$ M.

Finally, we showed the overview of the results at all KCl concentration. [Figure 4 – 6]

`

2. Leakage current

The dielectric gate oxide directly contacts with liquid channel, therefore, the electrochemical reaction at the interface is unavoidable. It is also the reason for leakage currents in the device. Furthermore the leakage currents are concerned to the robustness of the device. We also monitored gate currents which read from the gate electrode with ionic currents simultaneously.

Figure 4 – 7 tells the leakage currents certainly exist; however, the magnitude of leakage currents is 50 folds smaller than ionic current at least. Accordingly the gate voltage is dominated by capacitance increase of gate oxide. And the leakage currents are independent with concentration of KCl solution.

3. Conductance of nanochannels

To confirm the physical nanochannels radius, we calculated the conductance of nanochannels according to measured floating gate ionic current with variation of KCl concentration, and compared the theoretical calculation. In order to calculate the theoretical conductance of nanochannels, we should understand the structure of nanochannels which was fabricated by us. The cross section SEM image of nanochannels (one gate embedded region and two non – gated regions) and schematic image of nanochannels was illustrated in figure 3 – 7, 3 – 8, 3 – 9.

From the schematic image of nanochannels, we separated the nanochannels into one gate embedded region and two non – gated regions, and there were serial connection. The conductance of each part was denoted with G_1 (non – gated region), G_2 (gate embedded region), G_3 (non – gated region). For the convenience of calculation, we assumed the conductance of two non – gated regions were same ($G_1 = G_3$). Therefore, the total conductance of nanochannels was transformed from Equation 1 to Equation 2.

$$\frac{1}{G_{total}} = \frac{1}{G_1} + \frac{1}{G_2} + \frac{1}{G_3}$$ – Equation 1

`

$$G_{total} = \frac{G_1 G_2}{2G_2 + G_1} \text{ (when } G_1 = G_3) - \text{ Equation 2}$$

And the conductance of each part can be calculated with Equation 3.

$$G = n_0 q(\mu_{K^+} + \mu_{Cl^-}) \frac{A}{L} + \sigma_s \mu_{K^+} \frac{\pi d}{L} \text{ – Equation 3}$$

n_0 is bulk concentration, q is charge of electron, μ_{K^+} and μ_{Cl^-} are mobility of potassium ion and chlorine ion in electrolyte, A is cross section area of naonchannels, and L is the length of nanochannels.

From the SEM image, we could obtain the radius of nanochannels, gate embedded was 15 nm and non – gated region was 100 nm. And we have known the length of nanochannels already. In order to confirm the final unknown quantity – surface charge density (σ_s), we requested the zeta potential of Al_2O_3 at professional facility. With the result of measurement (zeta potential of Al_2O_3 is 4 mV.), we obtained the final surface charge density (σ_s) (-1.8 mC/m^2) through the Grahame Equation (Equation 4).

Figure 4 – 8 shows the results of conductance comparison with measurement and theoretical calculation. In the figure, we could find negligible conductance difference between 10^{-4} M and 10^{-5} M, because of EDL (Electric Double Layer) overlapping. And at harsh condition of 10^{-1} and 1 M condition, two results had discrepancy because of KCl precipitation in microchannels.

4. Ambipolar characteristics (relationship I_D with V_G)

Typically, for the case of SiO_2 based IFET (Ion Field Effect Transistor) has negative surface charges in neutral solution (pH 7), cations are naturally attracted to the surface for neutralize the negative charge, hence the cations exists in the nanochannel dominantly, and acts as major carriers in this system, the transistor is P type FET resultantly. Furthermore, due to the original surface charge density of SiO_2 is considerably larger than induced charge by gate voltage; the gate voltage cannot overcome the inherent properties to N type FET. It means that channel has

`

only one inherent polarity regardless of gate voltage – unipolar characteristics. On the contrary, our device not only negative gate voltage can induce negative surface polarity, the device acts as P type FET, also positive gate voltage can induce positive surface polarity, the device acts as N type FET.

At all range of concentrations (10^{-5} ~ 10^{-2} M), ambipolar characteristic (I_D vs V_G) were shown because of low original surface charge density of Al_2O_3 and all around gate embedded structure shows 5 times higher capacitance value than plane structure theoretically at least.

Therefore, we discussed on 10^{-5} M first. Figure 4 – 9 shows the absolute ionic current (for negative V_{SD}+, the actual value of ionic current would be decrease due to < - > sign.) with variation with gate voltage. The ambipolar characteristic (I_D vs V_G) were shown in the figure. In order to analyze more detail, we calculated the conductance of nanochannels with case of V_{SD} (Source – Drain Voltage) > 0 and V_{SD} (Source – Drain Voltage) <0. We have mentioned the reason of conductance difference was from measurement errors and other unexpected phenomena in anterior of this chapter. [Figure 4 – 10]

We calculated the conductance of nanochannels [Figure 4 – 11] and conductance change with gate voltage variation to confirm the gate effect [Figure 4 – 12] with all bulk concentrations.

5. Compare with previous works

Compare to previous IFET (Ionic Field Effect Transistor) [2, 3], the presenting IFET (Ionic Field Effect Transistor) exhibited more effective performance. The lower threshold voltage demanded to inverse the inherent polarity of nanochannels surface. The threshold voltage – V_{th} was defined as the voltage which could make the surface potential of nanochannels from existing value to 0 V. When the applied voltage is greater than V_{th}, the nanochannels will be able to overcome the inherent property, oppositely, the gate voltage dose not achieves the desired level, and the nanochannels will maintain the inherent property.

`

Using the relationship of voltage with camcatitance, Q =CV, we could calculate the threshold voltage of presenting system. At preceding paragraph, we had defined the V_{th} as make the surface potential is 0V. This means that the extra induced surface charge by gate voltage can offset the inherent surface charge to zero polarity. The Al_2O_3 used in this paper is only -1.8 mC/m^2. It's extremely low surface charge density compare to SiO_2. And because of all – around structure, the capacitance of gate oxide is 6.53 mF/m^2. And this value is 5 times higher than planar type gate electrode. Lower inherent surface charge added high capacitance, the V_{th} must be small than previous researches. We calculated the V_{th} of our system was only 0.23 V. [Equation 4, 5 used to calculate the capacitance.]

$$C_{ox} = \frac{\varepsilon_0 \varepsilon_r}{d_{die}} \quad - \text{Equation 4 (for planar type)}$$

$$C_{ox} = \frac{\varepsilon_0 \varepsilon_r}{r \ln(1+\frac{d_{die}}{r})} \quad - \text{Equation 5 (for cylinder type)}$$

C_{ox} is capacitance of oxide, ε_0 and ε_r are permittivity and dielectric constant of Al_2O_3, d_{die} is thickness of Al_2O_3, r is radius of nanochannels.

In Figure 4 – 13, the diagonal line represents connection of iso – surface charge points. Therefore, we chose two papers [1, 2] which described similar level of surface charge density (Ref. 1: -2 mC/m2, Ref. 2: ~3 mC/m2) to compare with our devices. As results, our device showed more effective performance than previous studied.

Finally, we compared the performance of gate effect with previous literatures. Because of the physical dimension difference, direct comparison was less meaningful. Anyway, our devices showed quite good when compared with others. And we chose one of them which had similar physical dimension with our devices to compared performance of gate effect. Table 4 – 14, 4 – 15 show the results of performance comparison.

`

6. Reference

[1]. Guan et al., Nat. Commun., **2**, 506 (2011).

[2]. Fan et al., Phy. Rev. Lett., **95**, 086607 (2005).

[3]. U.Vermesh et al., Nano Lett., **9**, No. 4, 1315 (2009).

[4]. R. Fan et al., Nature Materials **7**, 303 (2008).

`

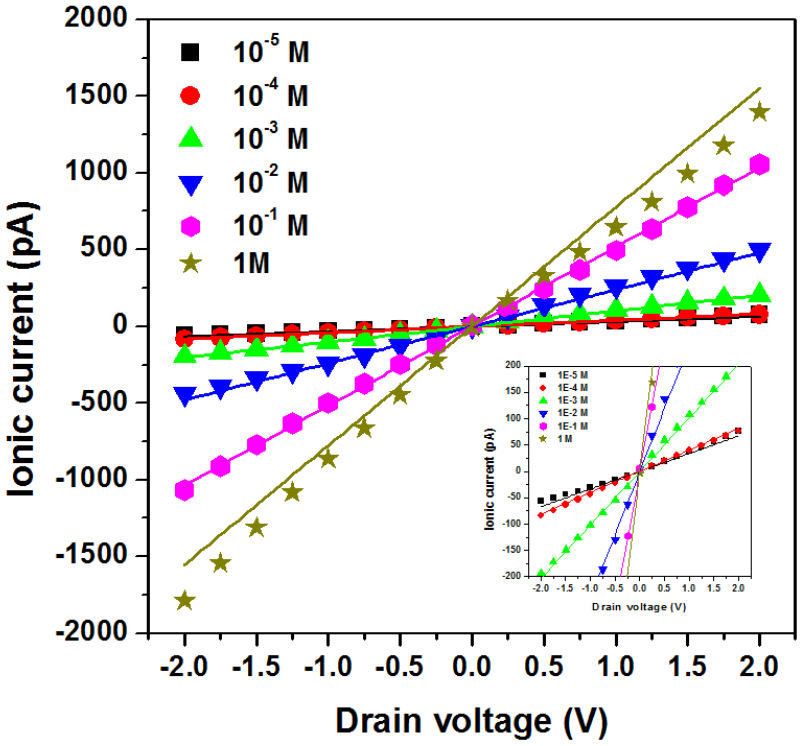

Figure 4 – 1: The floating gate ionic current with variation of KCl concentration.

Ionic current gave us ohmic behavior within range of V_{SD} (Source – Drain Voltage) = -2 ~ 2 V, and the bulk concentration was accompanied by an ionic current increase, because KCl concentration was equal with carrier concentration in the electrical circuit.

`

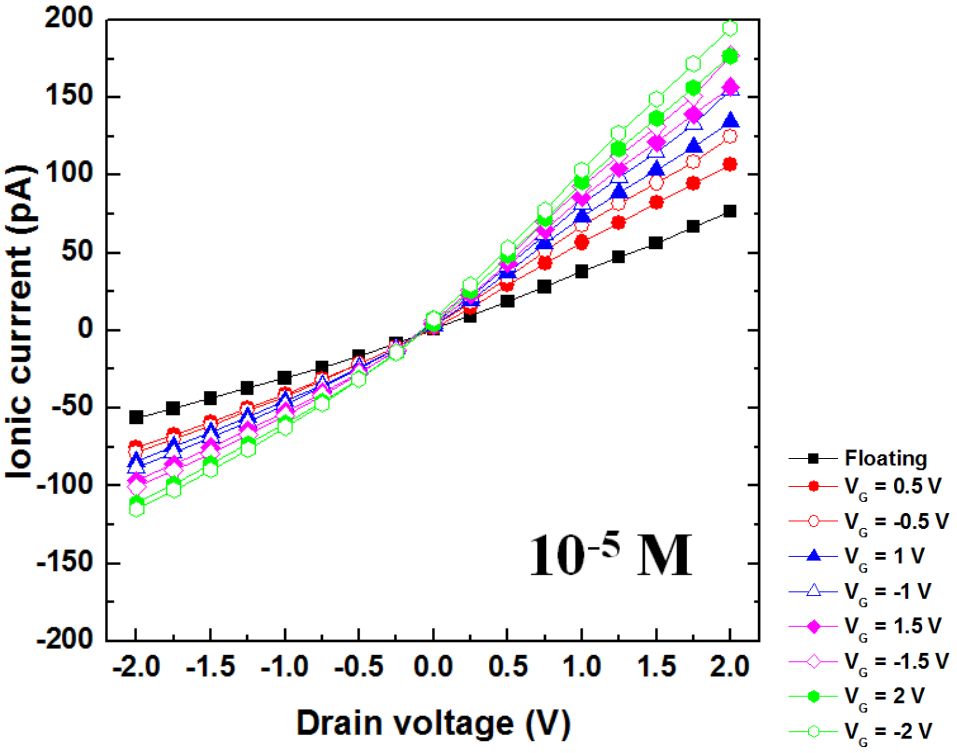

Figure Figure 4 – 2: At 10^{-5} M, the relationship I_D with V_{SD}.

Regardless of gate voltage polarity, the ionic current increased when gate voltage is applied. The difference of ionic current increase with V_{SD} (Source – Drain Voltage) bias may be caused by measurement errors and other unexpected phenomena.

`

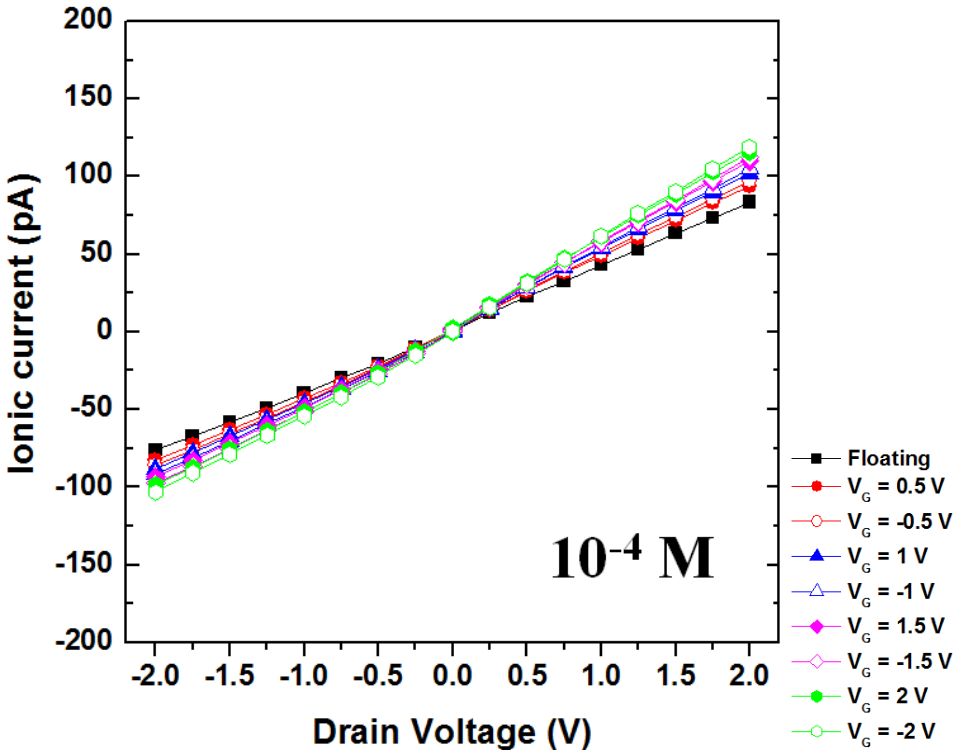

Figure 4 – 3: At 10^{-4} M, the relationship I_D with V_{SD}.

Regardless of gate voltage polarity, the ionic current increased when gate voltage is applied. The difference of ionic current increase with V_{SD} (Source – Drain Voltage) bias may be caused by measurement errors and other unexpected phenomena.

`

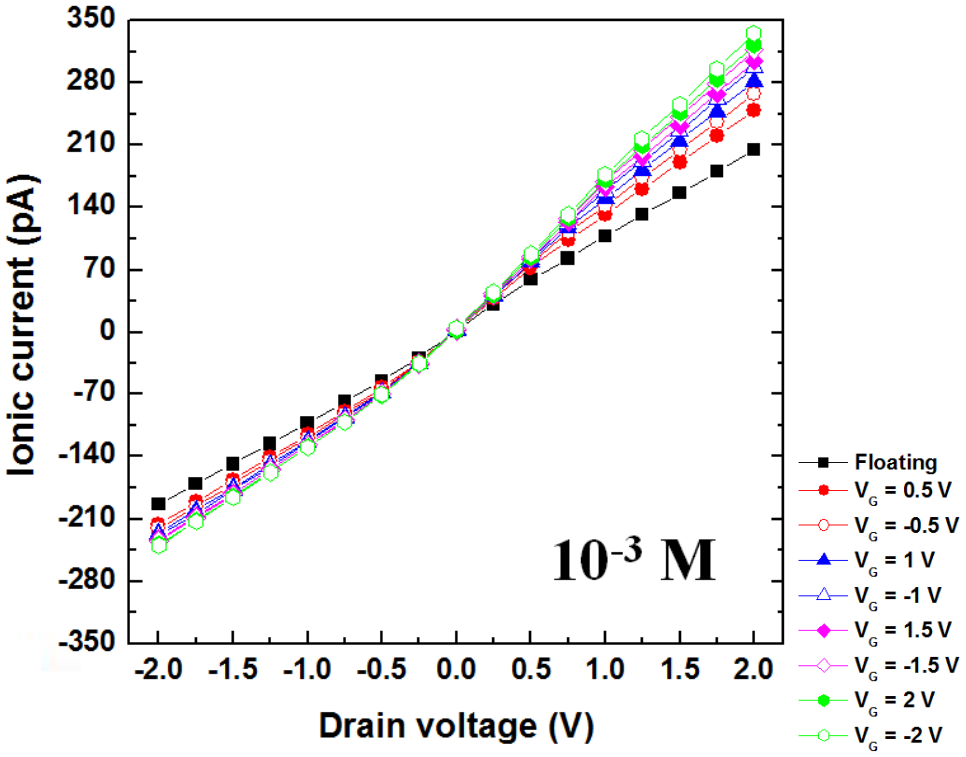

Figure 4 – 4: At 10^{-3} M, the relationship I_D with V_{SD}.

Regardless of gate voltage polarity, the ionic current increased when gate voltage is applied. The difference of ionic current increase with V_{SD} (Source – Drain Voltage) bias may be caused by measurement errors and other unexpected phenomena.

`

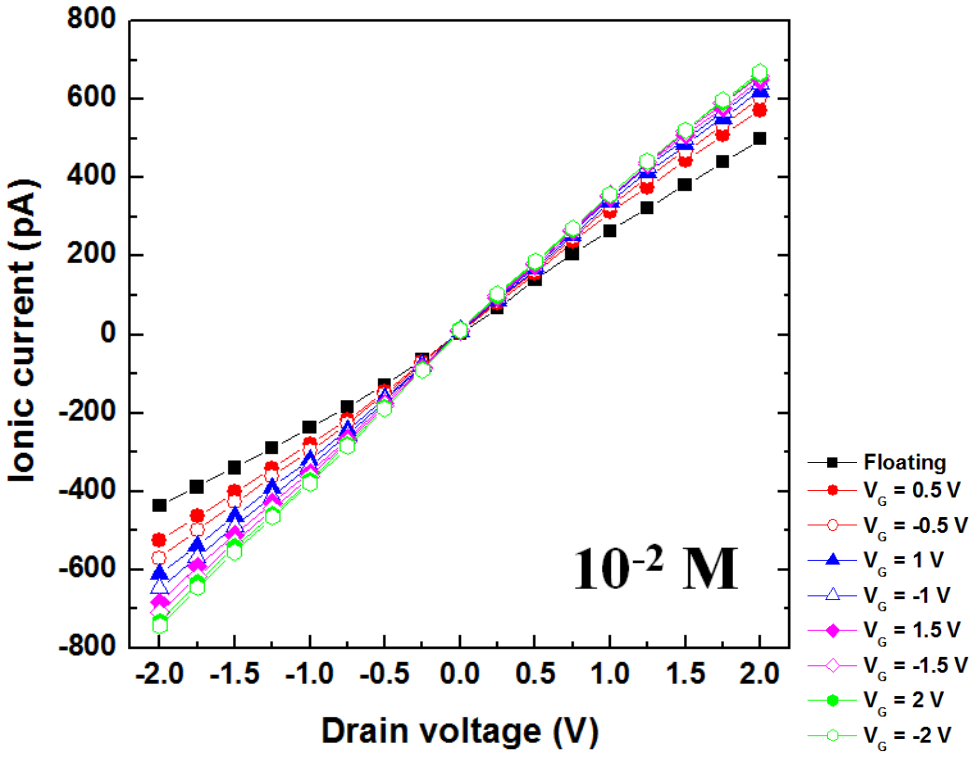

Figure 4 – 5: At 10^{-2} M the relationship I_D with V_{SD}.

Regardless of gate voltage polarity, the ionic current increased when gate voltage is applied. The difference of ionic current increase with V_{SD} (Source – Drain Voltage) bias may be caused by measurement errors and other unexpected phenomena.

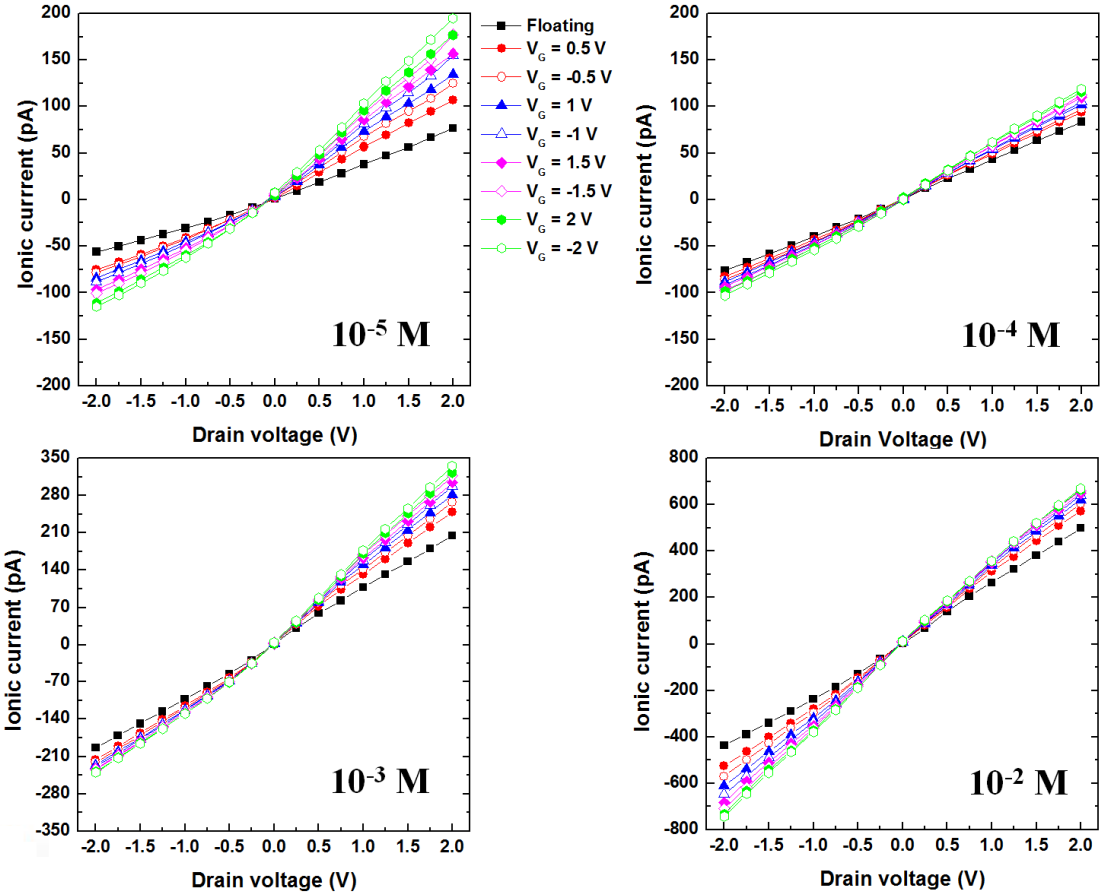

Figure 4 – 6: I_D vs V_D at all KCl concentration.

Overview of the results. The ionic current increased when gate voltage is applied and the device worked well with all KCl concentration. The trend of gate effect is identical with KCl concentration variation.

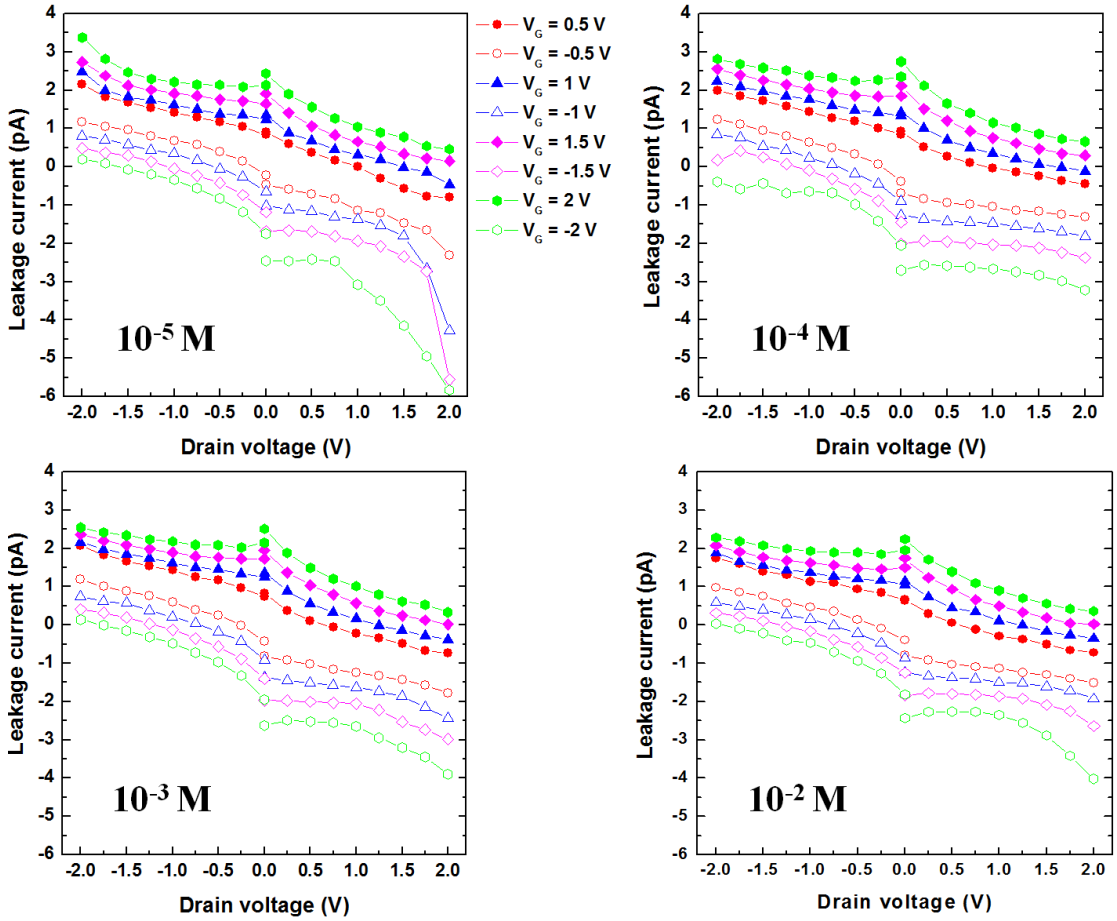

Figure 4 – 7: Leakage current at all KCl concentration.

In chapter of <Measurement>, Simultaneous measurement of currents is from drain voltage, gate voltage, and source voltage. The gate effect will be dominated by gate current (leakage current), however, the absolute value of gate current (leakage current) was only 50 times smaller, when compared with ionic current. With measurement of gate current (leakage current), we could confirm the robustness of our devices.

`

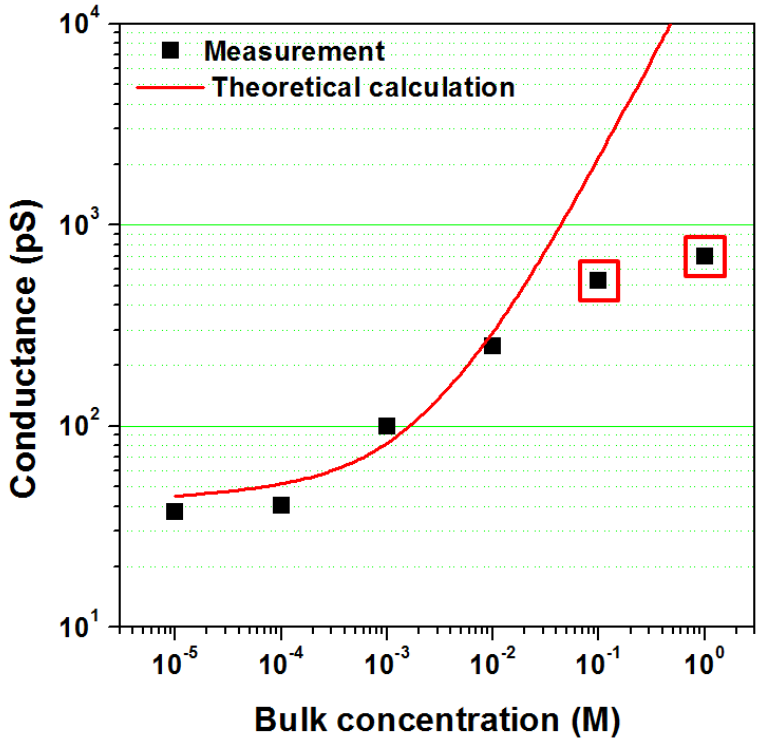

Figure 4 – 8: Compare two results of measurement and theoretical calculation.

The value of measurement and theoretical calculation was matched well each other. Negligible conductance difference was found between 10^{-4} M and 10^{-5} M, because of EDL (Electric Double Layer) overlapping. At harsh condition of 10^{-1} and 1 M condition, two results had discrepancy because of KCl precipitation in microchannels.

`

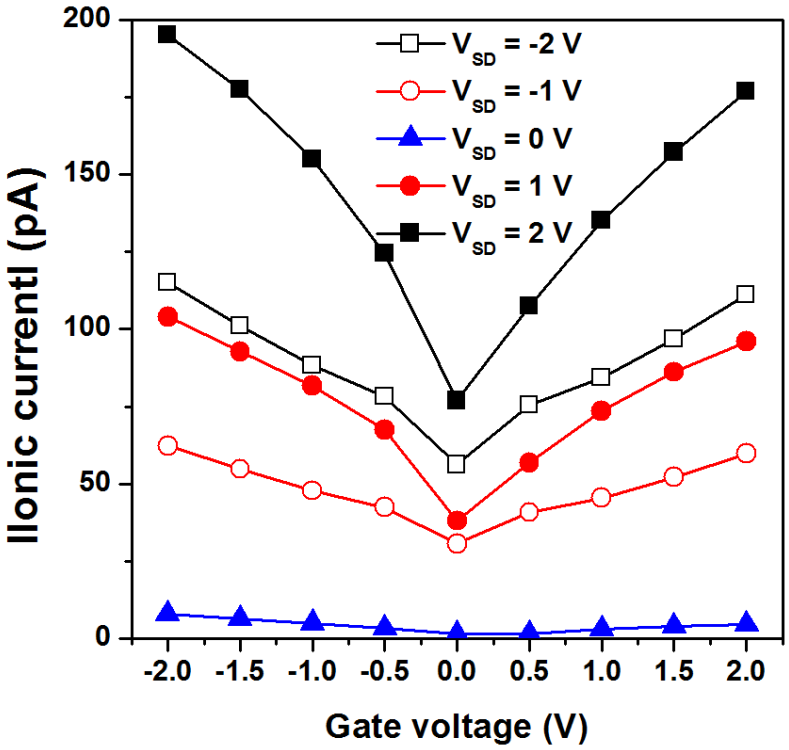

Figure 4 – 9: Absolute ionic current with variation with gate voltage.(10^{-5} M)

For negative VSD+, the actual value of ionic current would be decrease due to < - > sign. Thus we plotted the graph with absolute value. The figure shows clear ambipolar behavior compared with traditional IFET (Ionic Field Effect Transistor).

`

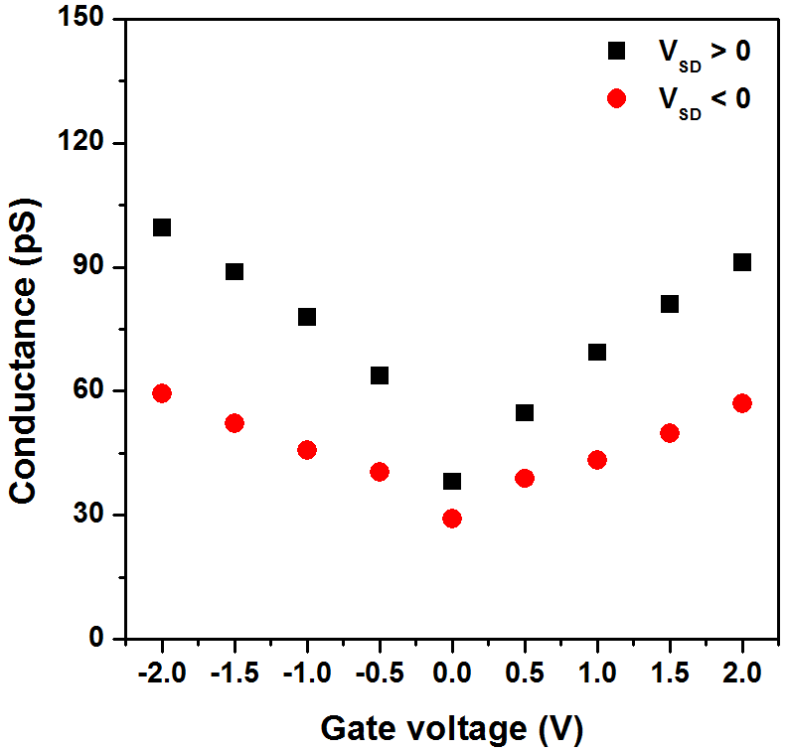

Figure 4 – 10: Conductance calculation with case of VSD (Source – Drain Voltage) > 0 and V_{SD} (Source – Drain Voltage) <0 . (10^{-5} M)

Conductance difference was from measurement errors and other unexpected phenomena.

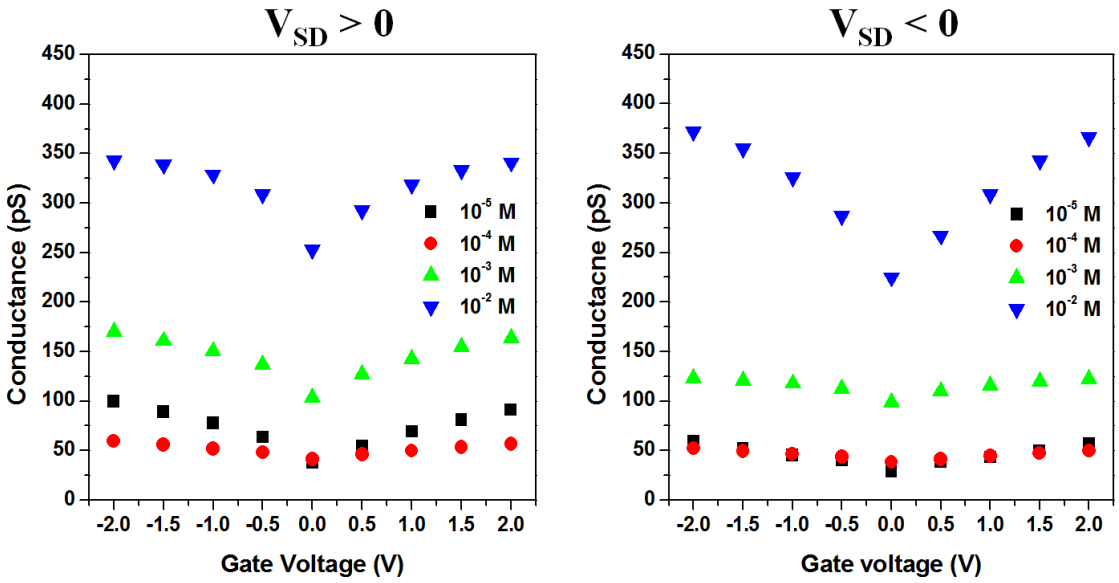

Figure 4 – 11: Conductance variation with bulk concentration.

Be same as overview of the results. The ionic current increase accompanied with nanochannels conductance increase. Negligible conductance difference was found between 10^{-4} M and 10^{-5} M, because of EDL (Electric Double Layer) overlapping.

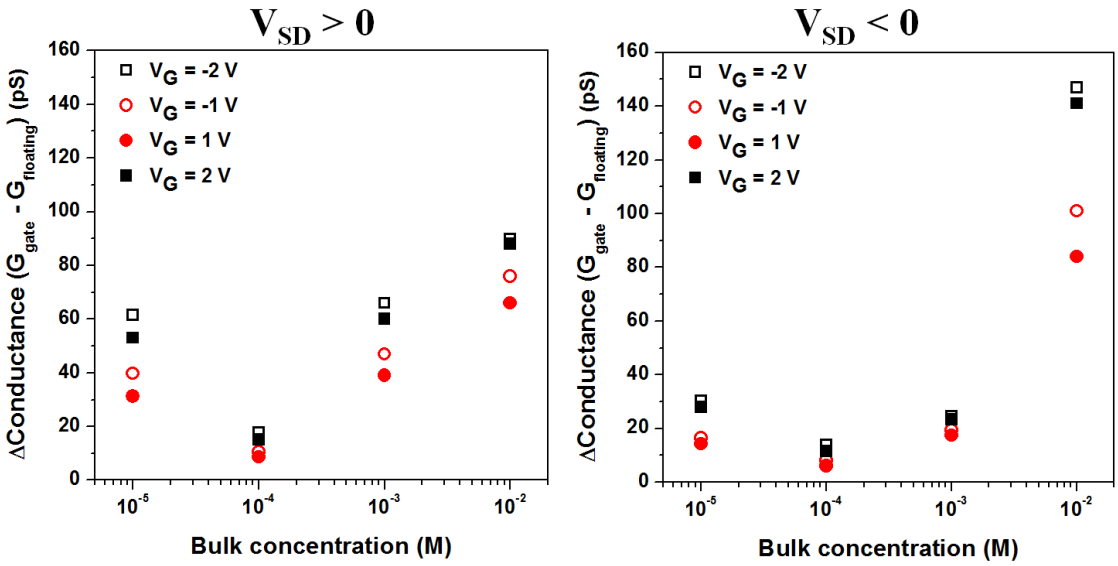

Figure 4 – 12: Conductance change with with gate voltage and bulk concentration.

The Conductance of nanochannels was increase increased by 1.5 ~ 3 times (absolute value: 10 ~ 150 pS) with gate voltage variation. Conductance increase was independent with the gate voltage polarity, which was different from traditional IFET (Ionic Field Effect Transistor).

`

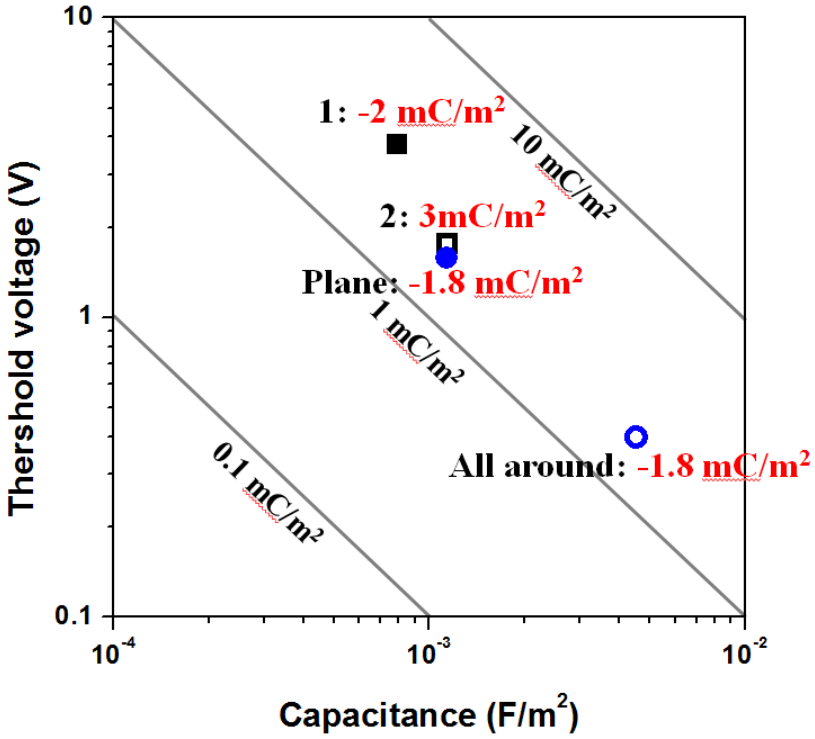

Figure 4 – 13: Threshold voltage comparison with published paper.

Because of capacitance, our device showed more efficient performance with similar surface charge density. Compare to planar type, cylindrical type exhibited more than 5 times capacitance value.

`

	SNU	Yale	Berkeley	Caltech	Berkeley
Dimension	Diameter: 15 nm Length: 10 μm (total 20 μm) No.: 80	Height: 20 nm Width: 22 μm Length: 100 μm	Diameter: ~8 nm Length: 22 μm No.: Mesoporous film (2 μm)	Diameter: 24 nm Length: 20 μm No.: 80	Diameter: 40~50 nm Length: 15 μm No.: 1
Cross section	1.3×10^4 nm^2	4.4×10^5 nm^2	50.24 << nm^2	3.6×10^4 nm^2	1590 nm^2
V_G	±2 V	-1.4 V	-1 V	-15 V	-10 V
$\frac{G_{Gate}}{G_{Floating}}$	1.5	1.5	1.7	1.3	1.2
Polarity	Ambipolar	Unipolar	Unipolar	Unipolar	Unipolar
Ref.		W. Guan et al. *Nature Communications* 2,506 (2011). [1]	R.Fan et al. *Phys. Rev. Lett.* **95** 086607 (2005). [2]	U.Vermesh et al. *Nano Lett.*, **Vol. 9**, No. 4, 1315 (2009). [3]	R. Fan et al. *Nature Materials* **7**, 303 (2008). [4]

Figure 4 – 14: Performance comparison

Because of physical dimension difference, direct comparison was hardly. In the table, our device shows quite good performance, and observed ambipolar behavior from our device only.

`

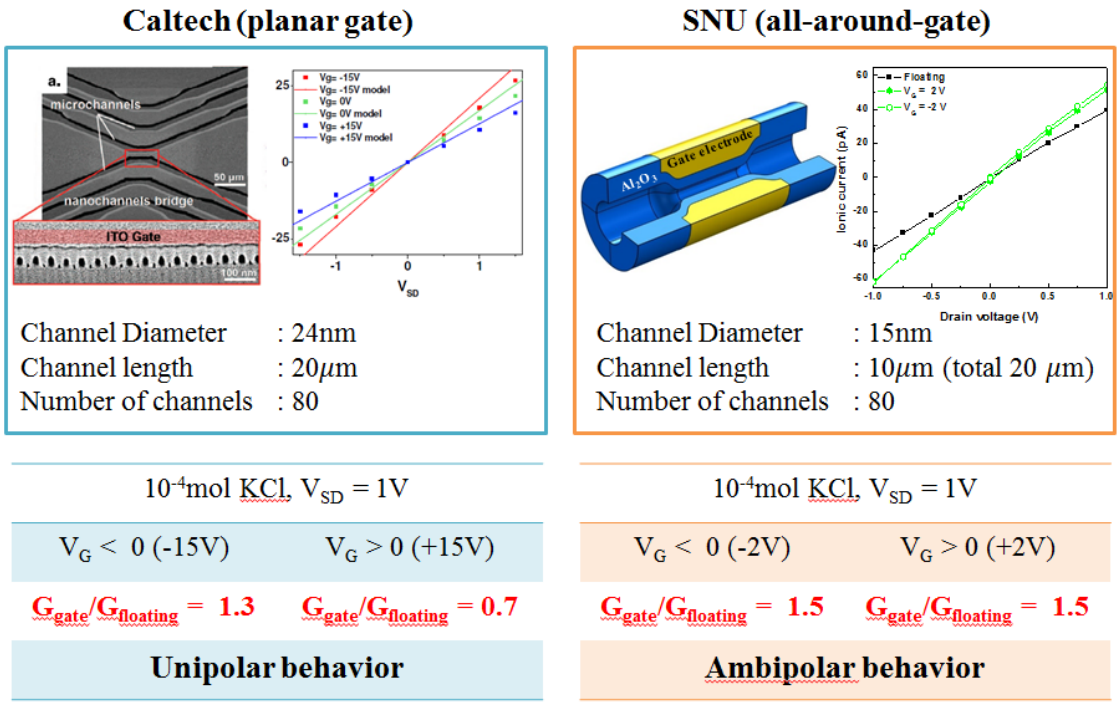

Figure 4 – 15: Performance comparison with Ref. 3.

With similar physical dimension, our device showed better performance than published paper.

`

Chapter 5. Computational simulation

`

5. Computational simulation

Two new phenomenological models of fringing effect and counter – ion condensation effect were adopted by us to analyze the partially gated IFET (Ion Field Effect Transistor) more accurately. When describing electrokinetics of nanofluidic systems including IFET (Ion Field Effect Transistor), previous researches were based on typical PNPS (Possion – Nernst – Plank – Stocks) model without any constraints. And the computational simulation was conducted by Mr. Hyomin Lee who was from Prof. Sungjae Kim.

1. Fringing effect

A typical capacitor is composed of two conductive objects with a dielectric material in between them. When a voltage difference applied between these objects, an electric field will be generated between them. And this electric field does not disappear abruptly at the edge of conductive objects, some of filed extend to beyond of edge of conductive objects. Typically, when a voltage is applied to gate electrode of partially gated IFET (Ion Field Effect Transistor), the generated electric field by gate voltage should be exist at the region of gate electrode embedded; oppositely, the induced electric field ought to disappear abruptly at non – gated region. Therefore, not only the oxide layer of gate embedded region can act as capacitor. Lin e*t al.* showed an experimental result of fringing effect using carbon nanotube FET (CNFET). [1], [Figure 5 – 1] With this experiment, we could prove the existence of fringing effect, but accurate mathematical model of fringing effect have not existed yet. To solve this problem, we developed phenomenological model to describe the effect. We assumed the gate voltage could modulate zeta potential of nanochannel with the Gaussian distribution. [Equation 1, 2, 3]

$f(x) = \frac{A}{\sigma\sqrt{2\pi}} exp[-\frac{(x-\mu)^2}{2\sigma^2}]$ – Equation 1

`

$$\zeta(z) = \begin{cases} \zeta_{gate} & \text{for gate embedded region – Equation 2} \\ \zeta_{gate} \exp\left[-\frac{\left(z \pm \frac{L_{gate}}{2}\right)^2}{\alpha^2}\right] & \text{for non – gated region – Equation 3} \end{cases}$$

A is an arbitrary constant, σ is the standard deviation, and μ is the mean value of the arbitrary function f(x). α^2 is defined as $\alpha^2 = (L_{channel} - L_{gate})^2/4ln\beta$, $L_{channel}$ is length of the nanochannel, and L_{gate} is length of gated region, $\beta = \zeta_{gate}/\zeta_{min}$, so β is constant which define the minimum zeta potential at the end of nanochannel.

We illustrated Figure 5 – 2 for modulated zeta potential scheme.

2. Counter ion condensation

In EDL (Electric Double Layer) part, we mentioned the Stern and Grahame model had biggest drawback was this model could not applied to highly charged surface. The critical potential is thermal voltage, RT/F≒25mV [2]. If the surface potential is greater than critical value, the classic model will breakdown to describe the electric double layer because of non – linearity. Under this condition of high surface potential, we should consider a new phenomenon is ion – ion interaction. Due to consideration of ion – ion interaction, the non – liner effect could be solved, but being such, an additional compact counter ion layer should be proposed. Consequently, a new compact layer is formed beyond the Stern layer, and the compact layer acts as additional Stern layer. Therefore, the number of ions would be contributed to ionic current decrease. Kilic e*t al.* developed the new analytical model to analyze the phenomena. We defined the parameter ν represents the ratio of bulk concentration (C_0) and the maximum condensed concentration (C_{max}) as [Equation 4], [2], [Figure 5 – 3]

$\nu = \frac{2C_0}{C_{max}} = 2a^3 N_A C_0$ – Equation 4 [2]

N_A is Avogadro constant, a is the effective diameter of ion, consider with ion – ion interaction.

`

Based on this parameter, we defined another parameter; critical potential φ_{cr} formed the non – linearity of the electrical double layer. [Equation 5]

$\varphi_{cr} = \frac{RT}{ZF} ln \frac{2}{\upsilon}$ – Equation 5 [2]

Then the charge and potential relation was separated in two forms depending on the critical potential [Equation 6, 7] [2]

$$\sigma_s = \begin{cases} 4ZFC_o\lambda_D \sinh\left(\frac{ZF\zeta}{RT}\right) & \text{at } |\zeta| \leq \varphi_{cr} \text{ – Equation 6} \\ 2sgn(\zeta)ZFC_o\lambda_D\sqrt{2/\upsilon}\sqrt{(1-\upsilon/2)^2 - ln\frac{\upsilon}{2} + \frac{ZF|\zeta|}{RT}} & \text{at } |\zeta| > \varphi_{cr} \text{ – Equation 7} \end{cases}$$

λ_D is the Debye screening length,

$$\lambda_D = \sqrt{\frac{k_B T \varepsilon_r \varepsilon_0}{2 z_i^2 e^2 n_i^{\infty}}}$$

Based on all of these informations, we obtained the numerical results were consistent with the measurement results. Figure 5 – 4, and 5 – 5 show the ionic current and conductance results each other.

`

3. Reference

[1]. Y. Lin et al., Nano Lett., **4 (5)**, 947–950, (2004).

[2]. Mustafa Sabri Kilic et al., Phys. Rev. E, **75**, 021502, (2007).

`

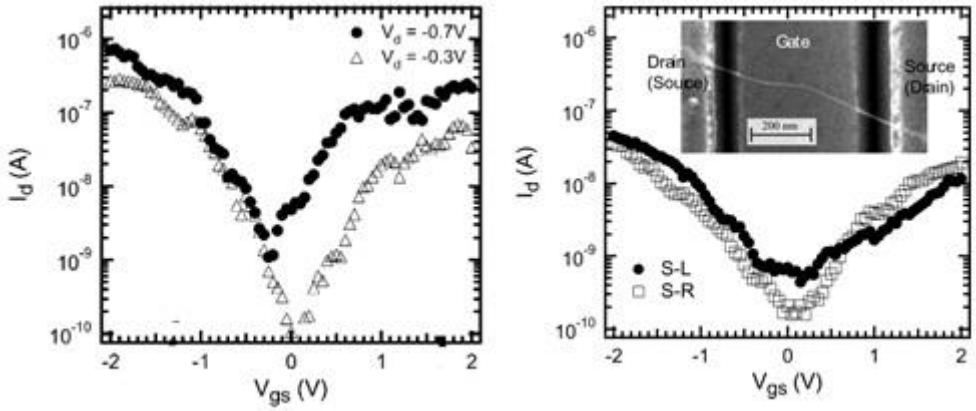

Figure 5 – 1: Effect of partially gated carbon nanotube FET.

The partially gated structure worked as fully gated structure in the electron devices. Thus, we referenced to the concept of fringing effect phenomena to our devices. [1]

`

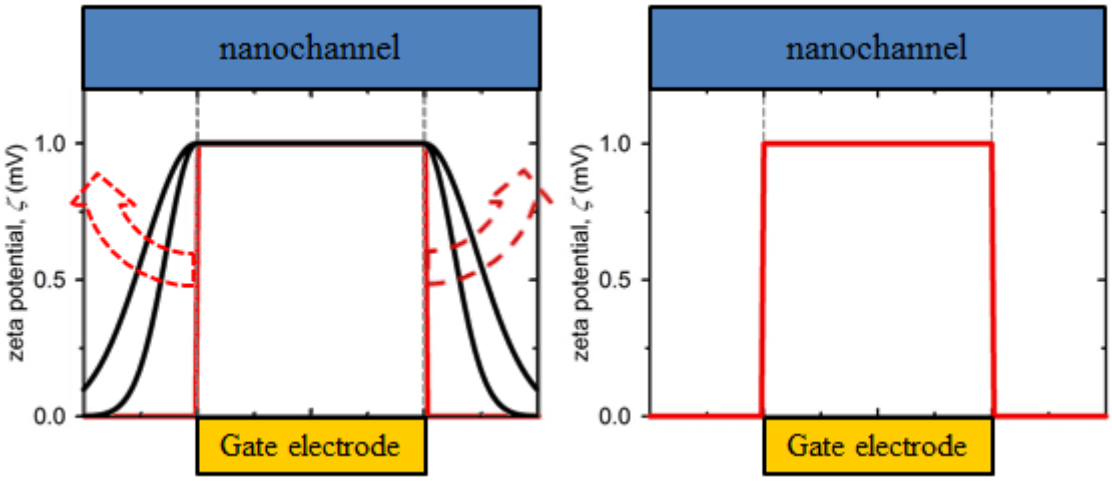

Figure 5 – 2: Modulated gate effect by fringing effect.

Same as electron devices, the gate voltage not only modulated zeta potential of gate embedded region, but also modulated zeta potential of non – gated region slightly. The degree of modulation of zeta potential at non – gated region was expressed by Gaussian distribution.

`

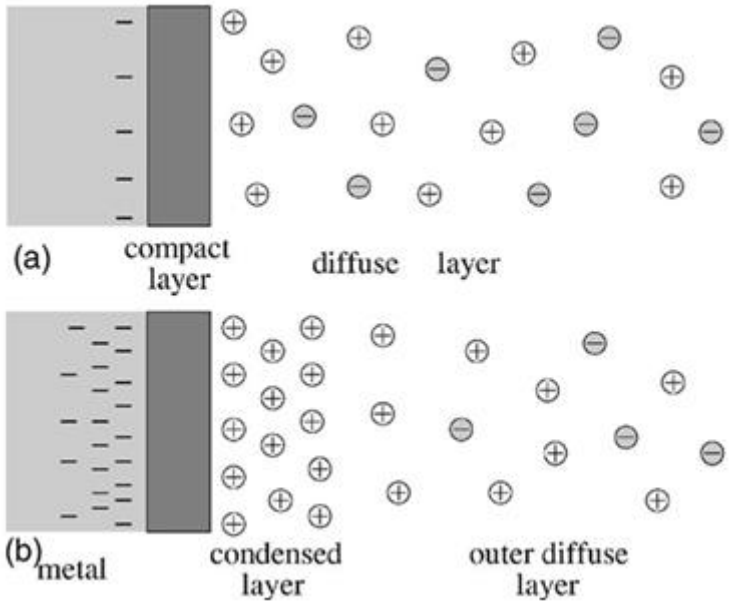

Figure 5 – 3: Concept of counter ion condensation effect.

The surface potential is greater than critical value [25 mV], the classic model will breakdown to describe the electric double layer because of non – linearity. We should consider ion – ion interaction to solve the non – liner effect. Since, an additional compact counter ion layer should be proposed.

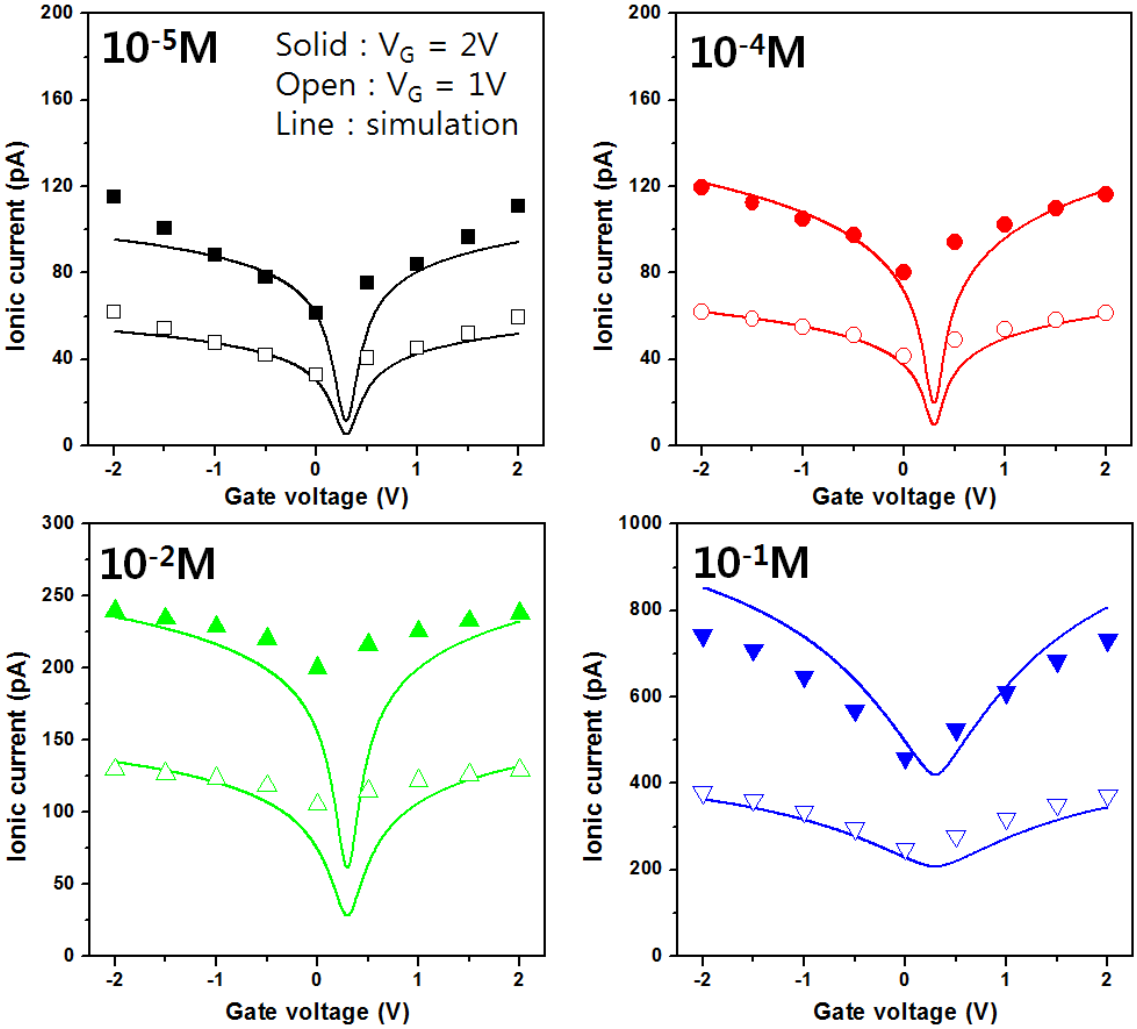

Figure 5 – 4: Comparison simulation results with measurement ones (ionic current).

Numerical results were consistent with the measurement results. Researcher should consider two additional constraints when they analyze the electronkinetics for partially gated IFET (Ionic Field Effect Transistor).

`

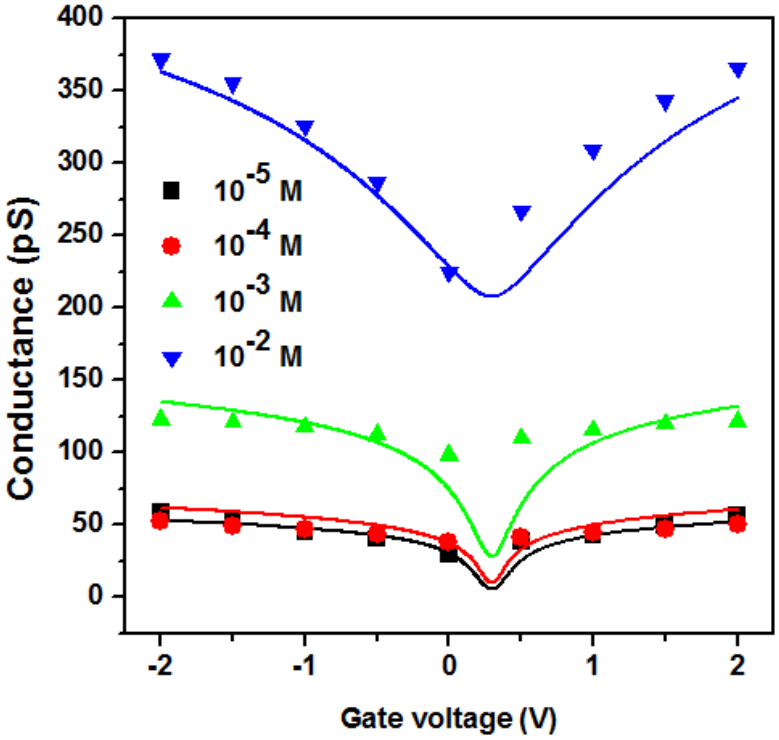

Figure 5 – 5: Comparison simulation results with measurement ones (ionic current).

Numerical results were consistent with the measurement results.

`

Chapter 6. Conclusion

`

6. Conclusion

With E-beam lithography and ALD (Atomic Layer Deposition) method were used to fabricate high aspect ratio (15 nm diameter, and 20 μm length) and well defined nanochannels. And using almost neutral (-1.8mC/m^2) Al_2O_3 dielectric gate oxide instead of high surface charge (-20 ~ -60mC/m^2) SiO_2. Solved the problems of surface polarity and low gate effect due to low dielectric constant simultaneously. (Dielectric constant of Al_2O_3 (9) is 2 times higher than SiO_2 (4.5). As a result, all-around type gate electrode enhanced with high dielectric constant material, the capacitance value of dielectric oxide about 5 times compared with planar type gate electrode.

Conductance of nanochannels was increased by 1.5 ~ 3 times (absolute value: 10 ~ 150 pS) with gate voltage variation and it was independent with the gate voltage polarity, which was different from traditional IFET (Ionic Field Effect Transistor). The devices showes ambipolar behavior which had not shown before. Moreover, experiment and simulation results were well matched using commercial software, COMSOL.

`

국문초록

반도체와 클린룸 기술의 발전에 따라서, 인류가 제작 가능한 소자는 나노미터 스케일까지 도달하면서 많은 신생사물들이 등장하게 되었다. 그 가운데 나노플루이딕스가 존재한다. 나노플루이딕스는 <나노테크놀로지>와 <플루이딕스> 의 합성어로, 두 개의 장점을 한 몸에 안고 있다. 이렇게 제작된 나노플루이딕스 소자는 생체분자 분석, 청정 에네지 생성과 같은 여러 분야에 사용되고 있다. 그리하여 지난 10 년간 이에 관하여 많은 연구가 진행되었다.

나노플루이딕스는 수용액 속에서 전하를 띈 입자, 특히 생체분자에 관한 연구에 많은 관심을 가지고 있다. 많은 생체분자는 수용액 상태에 존재하고 그 크기가 10 nm 미만이다. 그러므로 정확하게 나노미터 스케일을 가지는 플랫폼을 통하여 수용액 속에 있는 생체분자의 분석이 가능해 진다. 하지만 수용액 속의 생체분자를 컨트롤하려면 먼저 그 안에 있는 이온의 움직임부터 컨트롤 해야 한다.

이 논문에서는 all – around 게이트가 삽입된 이온트랜지스터를 제작하여, 그를 통하여 이온의 흐름을 컨트롤하였다. 특히, 소자의 제작에 있어서 10 nm 급의 채널 크기를 제작하는 공정 기술을 개발함과 아울러, 투명전극인 AZO (Al – doped Zinc Oxide) 을 gate 로 사용하였다. 그리고 유전상수가 실리콘 옥사이드의 2 배, 그리고 표면전하가 -1.8 mC/m^2 로, 거의 0 에 가까운 알루미늄 옥사이드를 사용함으로, 소자가 기존에 발표된 이온트랜지스터와는 달리 게이트의 극성과 관계없이 ambipolar 특성을 갖는 소자를 제작하였다.

그 이유는 게이트 구조와 알루미늄 옥사이드의 고유의 표면전하 양과 밀접한 관계가 있다. all – around 게이트 구조는 같은 유전상수와 두께를 가지는 planar 게이트 구조보다, 같은 게이트 전압에서 5 배 이상의 추가적인 표면전하를 생성할 수 있다. 그리고 논문에서 사용된 알루미늄 옥사이드의 표면이 거의 전하를 띄지 않고 있기 때문에, 그 극성을 더 쉽게 바꿀 수 있다. 이 소자로 수용액 농도 10^{-5} M 에서 10^{-2} M 까지 측정함으로써, 게이트 효과를 증명하였다.

`

그리고 측정결과를 COMSOL simulation 을 통하여 검증하였다. 게이트가 부분적으로 형성된 본 소자에서는 fringing field effect 와 counter ion condensation 이 일어나는 것을 간접적으로 증명하였다.

투명전극으로 사용되는 AZO (Al – doped Zinc Oxide) 를 게이트로 사용하였기 때문에, 생체분자의 흐름을 전기적으로 컨트롤하고, 광학으로 동시에 관찰가능한 소자이다. 이런 점에서 볼 때, 이 소자는 앞으로 생체분자 분석에 아주 유용한 툴로 사용될 것이다.

Keywords: Nanofluidics, Nanochannel, Ionic field effect transistor

Student number: 2012-23926